Chapter 9
Computer-Aided Analysis of Acousto-Optic Interactions

9.1 INTRODUCTION

The photoelastic matrix **p** is as fundamental to the analysis of the A/O interaction as the stiffness matrix is to the propagation of acoustic waves. Its form is identical to the piezo-optic matrix considered in Chapter 7, and is used when strain rather than stress is the independent variable (i.e., in the interaction of light with acoustic waves). The components of **p** determine the magnitude of the diffracted light for a particular interaction geometry and thus determine the figure of merit (FOM) for the interaction. The FOM in conjunction with the Bragg and acoustic bandwidths and the frequency resolution completely specify the A/O interaction. Thus, the photoelastic constants play a critical role in determining device performance. A strong interaction, for example, allows the device designer the freedom to reduce the transducer length (for a given H), which increases the Bragg bandwidth. Conversely, a weak interaction may require increasing L/H and decreasing either the bandwidth or the resolution. The photoelastic components, like the indices of refraction, exhibit dispersion and must be specified at a particular optic wavelength.

Just as the effective stiffness constant can be determined in many situations by inspection of the stiffness or the Christoffel matrices, it is possible to find the effective photoelastic constant p_{eff} by inspection of **p**, but only in the simplest interaction geometries. The reason is that the evaluation of p_{eff} requires attention not only to the acoustic and optic propagation directions but also to the acoustic and optic polarizations. In many cases, changing the optic polarization transforms a weak interaction into a strong interaction. In this chapter, we develop the tools to evaluate p_{eff} for arbitrary directions of the (four) relevant interaction parameters: the directions of the optic and acoustic waves and their polarizations. We investigate a number of the configurations discussed in Chapter 8, including the isotropic and birefringent interactions in lithium niobate ($LiNbO_3$) and paratellurite (TeO_2), and the isotropic interaction in gallium phosphide (GaP). In addition, we consider a two-dimensional geometry using GaP, which may prove useful in some newer applications.

9.2 ACOUSTO-OPTIC INTERACTIONS IN ISOTROPIC AND CUBIC SYSTEMS

The simplest case is the interaction in an isotropic body. The photoelastic matrix contains two independent components and is given by

$$\mathbf{p} = \begin{bmatrix} p_{11} & p_{12} & p_{12} & 0 & 0 & 0 \\ p_{12} & p_{11} & p_{12} & 0 & 0 & 0 \\ p_{12} & p_{12} & p_{11} & 0 & 0 & 0 \\ 0 & 0 & 0 & p_{44} & 0 & 0 \\ 0 & 0 & 0 & 0 & p_{44} & 0 \\ 0 & 0 & 0 & 0 & 0 & p_{44} \end{bmatrix} \tag{9.1}$$

where

$$p_{44} = \frac{p_{11} - p_{12}}{2} \tag{9.2}$$

Equation (9.2) is the "isotropy" condition for the photoelastic matrix, and follows from the invariance of **p** for a 45° rotation about any principal axis. The form of the photoelastic matrix for cubic classes is similar to (9.1) without the isotropy condition. It possesses at least three independent components (as does the stiffness matrix for cubic symmetry). A further complication is that **p** is not required to be symmetric. Thus, for the cubic classes 23 and $m3$, $p_{12} \neq p_{21}$ (and **p** possesses four independent components). The important classes $\bar{4}3m$, 432, and $m3m$ are symmetric, however. The stiffness matrix for cubic classes has three independent components, because the off-diagonal symmetry does exit.

Given the form of the photoelastic matrix, we can write the perturbation to the index ellipsoid, using (7.26). There are six components to $\Delta\mathbf{B}$ corresponding to the six strain components:

$$\Delta\mathbf{B} = \mathbf{p}{:}\mathbf{S} \tag{9.3}$$

The full, perturbed index ellipsoid is given by (7.28):

$$B_{ij}\, x_i x_j = 1 \tag{9.4}$$

where

$$\mathbf{B} = \mathbf{B}^0 + \Delta\mathbf{B}$$

where $\mathbf{B}^0$ is the unperturbed component n_0 and $\Delta\mathbf{B}$ is given by (9.3). For cubic symmetry, (9.4) becomes

$$\frac{x^2 + y^2 + z^2}{n_o} + \Delta B_1 x^2 + \Delta B_2 y^2 + \Delta B_3 z^2 + \Delta B_4 yz + \Delta B_5 xz + \Delta B_6 xy = 1 \tag{9.5}$$

In (9.5),

$$B_1^0 = B_2^0 = B_3^0 = \frac{1}{n_o^2}$$

and (from (9.1) and (9.3))

$$\begin{aligned} \Delta B_1 &= p_{11}S_1 + p_{12}(S_2 + S_3), &\quad \Delta B_4 &= 2p_{44}S_4 \\ \Delta B_2 &= \overset{p_{11}}{\cancel{p_{12}}}S_2 + p_{12}(S_1 + S_3), &\quad \Delta B_5 &= 2p_{44}S_5 \\ \Delta B_3 &= p_{11}S_3 + p_{12}(S_1 + S_2), &\quad \Delta B_6 &= 2p_{44}S_6 \end{aligned}$$

Generally, there will be only *one* acoustic wave in any given situation, and thus it is more convenient to write (9.5) as six equations, one for each strain component. If more than one strain is present, each may be treated separately:

$$\begin{aligned}
S_1&:\quad x^2\left(\frac{1}{n_o^2} + p_{11}S_1\right) + y^2\left(\frac{1}{n_o^2} + p_{12}S_1\right) + z^2\left(\frac{1}{n_o^2} + p_{12}S_1\right) = 1 \\
S_2&:\quad x^2\left(\frac{1}{n_o^2} + p_{12}S_2\right) + y^2\left(\frac{1}{n_o^2} + p_{11}S_2\right) + z^2\left(\frac{1}{n_o^2} + p_{12}S_2\right) = 1 \\
S_3&:\quad x^2\left(\frac{1}{n_o^2} + p_{12}S_3\right) + y^2\left(\frac{1}{n_o^2} + p_{12}S_3\right) + z^2\left(\frac{1}{n_o^2} + p_{11}S_3\right) = 1 \\
S_4&:\quad \frac{x^2 + y^2 + z^2}{n_o^2} + 2p_{44}S_4 yz = 1 \\
S_5&:\quad \frac{x^2 + y^2 + z^2}{n_o^2} + 2p_{44}S_5 xz = 1 \\
S_6&:\quad \frac{x^2 + y^2 + z^2}{n_o^2} + 2p_{44}S_6 xy = 1
\end{aligned} \tag{9.6}$$

In (9.6), the variables are the principal axes of the index ellipsoid and thus represent *optic* polarization directions. (The presence of the 2 in the shear terms of (9.6) is due to the symmetry of the impermeability matrix, and occurs for all cross terms in the perturbed indicatrix.) We assume that the perturbed acoustic wave corresponds to one of the six strains in the crystal axis system. Thus S_1, S_2, and S_3 represent longitudinal waves propagating along the x, y, and z Cartesian axes, and S_4, e.g., corresponds either to a y-polarized, z-propagating or to a z-propagating, y-polarized shear wave. If the acoustic perturbation is an "off-axis" mode, the perturbed index ellipsoid will consist of combinations of equations in terms of the principal strains. We can formulate the problem by using one equation if we *rotate* the crystal axes so that they conform to the orientation of the acoustic strain. Generally, this procedure requires a computer solution, which we consider later.

For a longitudinal acoustic wave propagating along the x-axis, the strain is given by S_1. From the first equation of (9.6), if the wave interacts with an x-polarized optic beam (parallel to the acoustic beam) incident along the y- or z-axis, the relevant term from (9.6) is

$$x^2\left(\frac{1}{n_o^2} + p_{11}S_1\right)$$

and the photoelastic constant of the interaction is simply p_{11}. The geometry for this interaction is shown in Figure 9.1(a). The photoelastic constant does not change as the optic beam is rotated around the acoustic beam as long as the polarization remains in the x direction (this is true for all classes). Note that for all optic beam directions the optic and acoustic polarizations are parallel. If the optic *polarization*, on the other hand, is rotated (for the z-incident beam) to the y-axis, the relevant term is

$$y^2\left(\frac{1}{n_o^2} + p_{12}S_1\right)$$

and the photoelastic constant is p_{12}.

If the *laser* is now rotated around the acoustic beam to the y-axis, the optic beam will be z-polarized, as in Figure 9.1(b). In this case, the optic and acoustic polarizations are perpendicular. The effective photoelastic constant is still p_{12} because of the cubic symmetry in which $p_{13} = p_{12}$ (generally this will not be true). Indeed, for arbitrary optic incidence in the yz plane, it is clear that $p_{\text{eff}} = p_{12}$. For any direction of optic incidence (in the yz plane), if the polarization is rotated from parallel to normal to

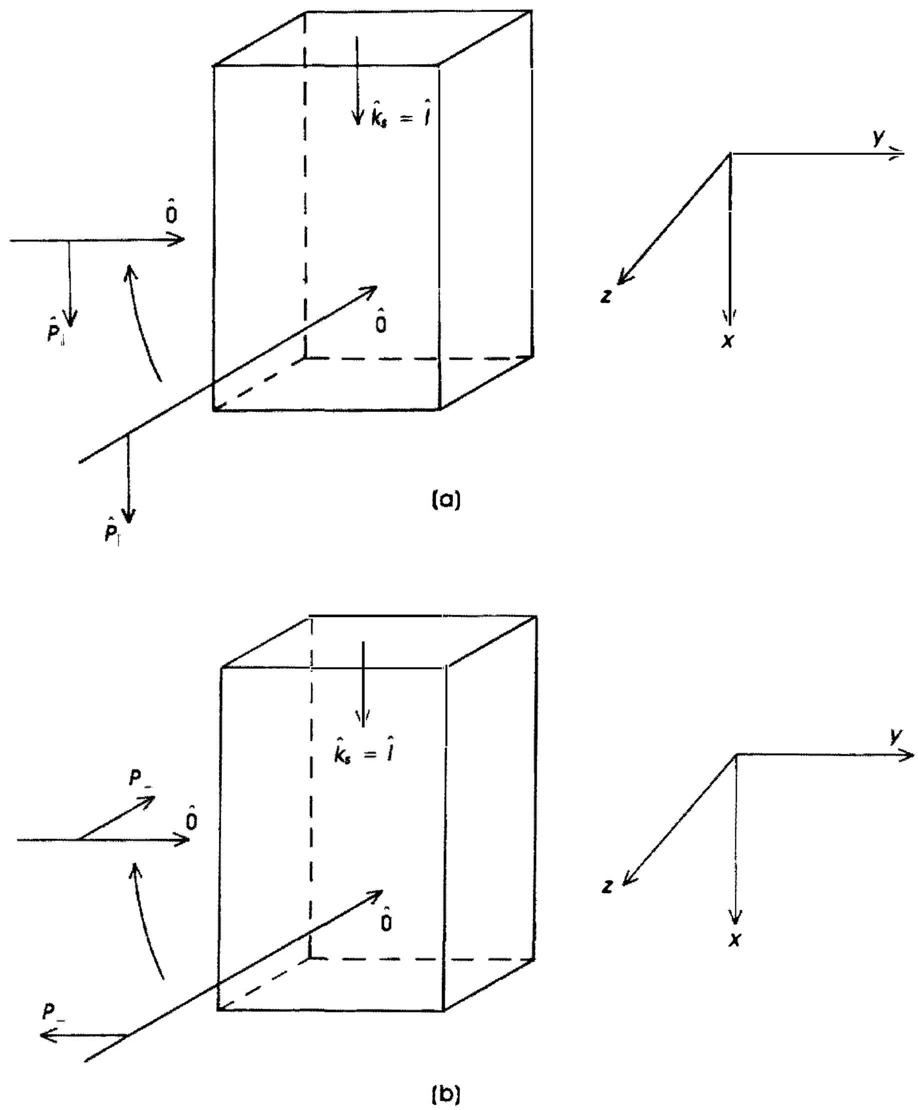

Figure 9.1 Configurations of A/O interactions in which the optic beam is (a) parallel and (b) perpendicular to the acoustic propagation direction.

the acoustic beam the effective photoelastic constant will change from p_{11} to p_{12}. These results are summarized in Figure 9.2. For a randomly polarized optic beam, the effective photoelastic constant is just the average of p_{11} and p_{12}.

Now consider the shear wave interaction S_4 (a y-propagating acoustic wave polarized in the z direction). The relevant term in (9.6) is

$$\frac{y^2 + z^2}{n_o^2} + 2p_{44}S_4yz = 1$$

The presence of the "cross" term in the perturbation immediately identifies the interaction as polarization flipped, in which the incident and diffracted waves are polarized orthogonally to each other. For an optic wave incident along the x-axis and polarized along z, the diffracted wave will be polarized along y. Conversely, if the incident beam is polarized along y, the diffracted beam will be z-polarized. In both these cases, the effective photoelastic constant is $2p_{44}$. The geometry of this interaction is shown in Figure 9.3(a). If, however, the optic wave is incident along the z-axis, the interaction requires coupling between the x- and z-polarized modes, which cannot occur with shear wave S_4. In general, an acoustic wave cannot cause a "flip" between optic polarizations that are both normal to acoustic polarization. Such an interaction, shown in Figure 9.3(b), is invalid and has a zero photoelastic constant. Similarly, an optic beam incident along y cannot interact with S_4 (this interaction in which the accoustic and optic beams are parallel is called a *collinear* interaction). Because all acoustic directions are equivalent for isotropic media, we can summarize the preceding results as follows:

1. For an acoustic longitudinal mode interacting with an optic polarization parallel to the acoustic wave, the photoelastic constant is p_{11}; for a normal optic polarization, it is p_{12};

2. For an acoustic shear wave, the effective photoelastic constant is $p_{44} = (p_{11} - p_{12})/2$ if the optic and acoustic polarizations are parallel, and zero if the optic incidence is parallel to the acoustic polarization. In addition, there are collinear interactions with shear waves. For fused quartz, the photoelastic components are $p_{11} = .12$ and $p_{12} = .27$. The FOM for a longitudinal wave (for the stronger perpendicular interaction) is

$$M_2 = \frac{n^6p^2}{\rho v_a^3} = \frac{1.47^6 \times .27 \times 10^2}{(2.2 \times 10^3)(5.96 \times 10^3)^3} = 1.6 \times 10^{-15}\ \mathrm{s^3/kg}$$

In determining the units of M_2, we use the fact that both n and p are dimensionless. Because of the importance of fused quartz in the optic

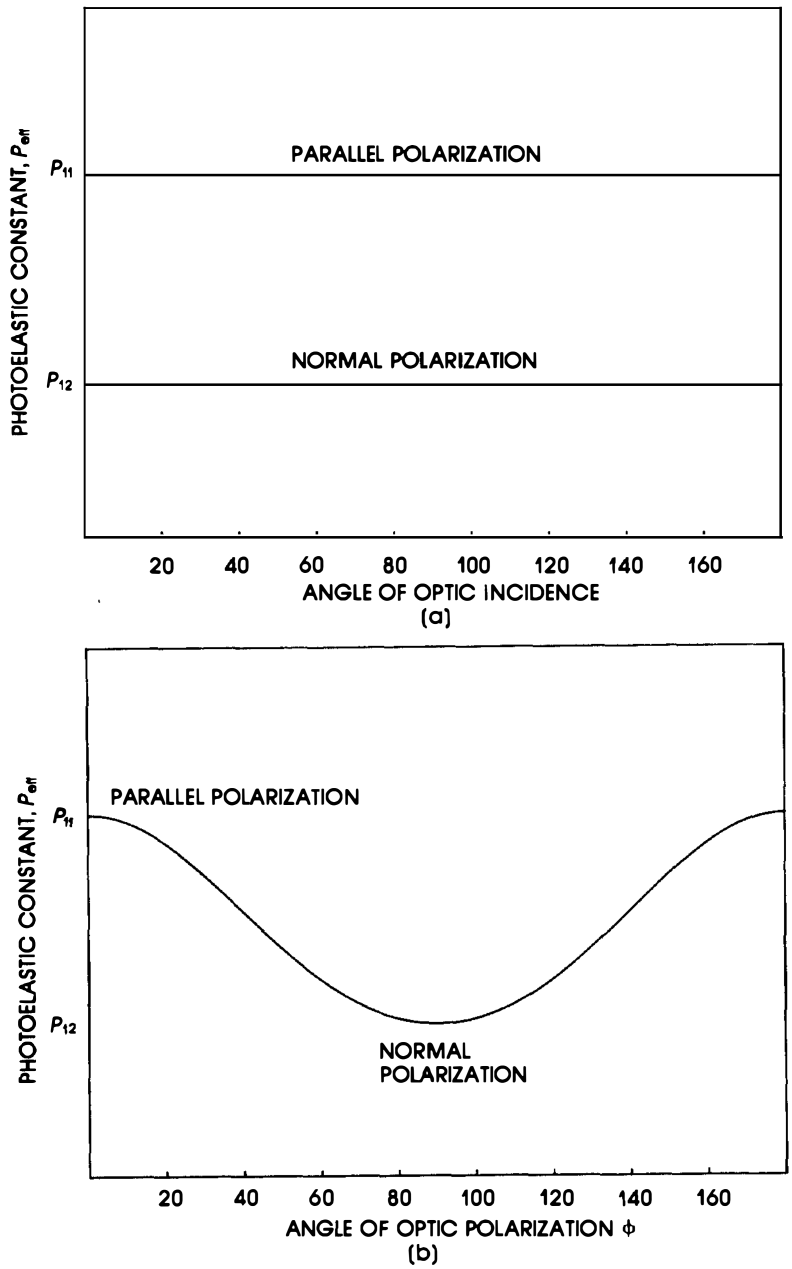

Figure 9.2 Dependence of the photoelastic constant of cubic crystal on (a) angle of incidence of optic beam and (b) direction of optic polarization. (*Note*: $\phi = 0$ corresponds to parallel polarization and $\phi = 90°$ corresponds to normal polarization.)

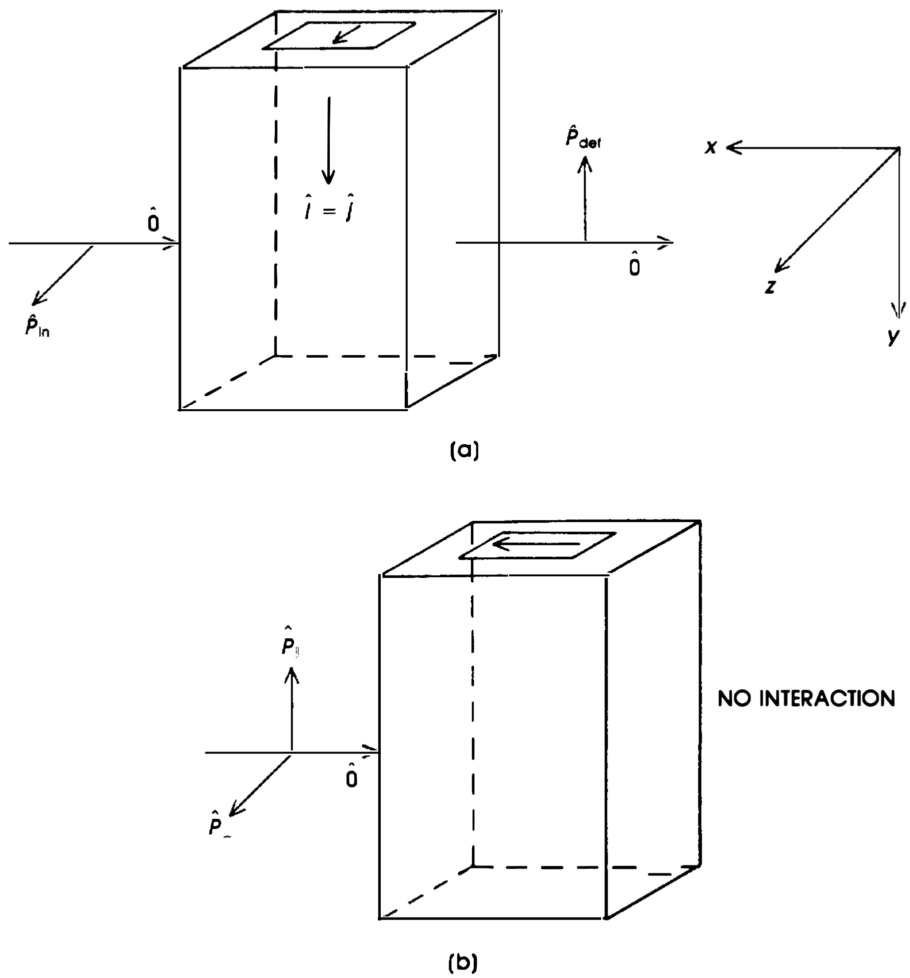

Figure 9.3 Determination of the effective photoelastic constant for shear interaction in cubic or isotropic systems. (a) The maximum interaction occurs when the optic incidence is normal to the acoustic polarizations. (b) No interaction occurs if the incidence is parallel to the acoustic polarization.

industry it is used as a standard even though it possesses relatively poor A/O performance.

In cubic symmetry, these results are valid for an acoustic wave propagating along the principal axes. Off-axis acoustic modes require somewhat more sophisticated analysis, which we consider later. In our discussion of the stiffness matrix, we mentioned that for cubic symmetry physical principles require $c_{11} > c_{12}$. No such constraint exists for the photoelastic components (in the cubic classes), and thus for a longitudinal wave the optimal interaction for one material may require a parallel optic polarization, yet for a similar crystal the interaction is stronger for normal optic polarization.

9.3 TETRAGONAL INTERACTIONS

The form of the photoelastic matrix for the symmetry classes $4/mm$, $\bar{4}2m$, 422, and $4mm$ is

$$\mathbf{P} = \begin{vmatrix} p_{11} & p_{12} & p_{13} & 0 & 0 & 0 \\ p_{12} & p_{11} & p_{13} & 0 & 0 & 0 \\ p_{31} & p_{31} & p_{33} & 0 & 0 & 0 \\ 0 & 0 & 0 & p_{44} & 0 & 0 \\ 0 & 0 & 0 & 0 & p_{44} & 0 \\ 0 & 0 & 0 & 0 & 0 & p_{66} \end{vmatrix} \tag{9.7}$$

Compared with the stiffness matrix in these classes, which possess six independent constants, the photoelastic matrix possesses seven because $p_{13} \neq p_{31}$. In the remaining tetragonal classes, there are 10 independent components (compared with 7 in the stiffness matrix for the same classes). The unperturbed indicatrix is an ellipsoid of revolution about the z (optic) axis, and thus all terms with z are written with n_e (extraordinary polarization). Of the six equations of (9.6), those for the S_1 and S_2 acoustic modes are identical, as are those for S_4 and S_5 (reflecting the fact that the x- and y-axes are identical). We write only four perturbed index equations:

$$\begin{aligned} S_1&: \quad x^2\left(\frac{1}{n_o^2} + p_{11}S_1\right) + y^2\left(\frac{1}{n_o^2} + p_{12}S_1\right) + z^2\left(\frac{1}{n_e^2} + p_{31}S_1\right) = 1 \\ S_3&: \quad x^2\left(\frac{1}{n_o^2} + p_{13}S_3\right) + y^2\left(\frac{1}{n_o^2} + p_{13}S_3\right) + z^2\left(\frac{1}{n_e^2} + p_{33}S_3\right) = 1 \\ S_4&: \quad \frac{x^2 + y^2}{n_o^2} + \frac{z^2}{n_e^2} + 2p_{44}S_4yz = 1 \\ S_6&: \quad \frac{x^2 + y^2}{n_o^2} + \frac{z^2}{n_e^2} + 2p_{66}S_6xy = 1 \end{aligned} \tag{9.8}$$

For the longitudinal wave S_1 interacting with an optic beam incident in the yz plane and polarized along x (the parallel case), $p_{\text{eff}} = p_{11}$ (as for cubic and isotropic symmetries). In the perpendicular case, if the optic beam is incident along y and polarized along z, then $p_{\text{eff}} = p_{31}$; but if the beam is incident along z and polarized along y, then $p_{\text{eff}} = p_{12}$. For the z-propagating longitudinal wave S_3, the parallel interaction has $p_{\text{eff}} = p_{33}$, whereas for the perpendicular interaction $p_{\text{eff}} = p_{13}$ for arbitrary optic incidence in the xy plane. In this case, the polarization is also in the xy plane (the index is thus n_o). The shear mode interactions are similar to the isotropic and cubic symmetries.

For S_4 or S_5, optic polarizations parallel to the acoustic polarization result in a photoelastic constant of p_{44}, whereas for S_6, $p_{\text{eff}} = p_{66}$. For optic polarizations normal to the acoustic polarization, there is no interaction. An important distinction in this symmetry is that for the S_4 and S_5 shear modes, the polarization flip is between the y (or x) and the z optic polarizations. Because the tetragonal system is optically uniaxial, the z index is generally different from the x or y indices, and thus the S_4 and S_5 interactions are birefringent and the S_6 interaction is not (because the "flip" is between the x- and y-axes).

Notice that the birefringent nature of these interactions is not contained explicitly in the interaction equations.

Example 9.1. Calculate the effective photoelastic constants and the optimal FOM M_2 for the following A/O interactions with TeO_2:

1. x-propagating longitudinal mode,
2. z-propagating longitudinal mode,
3. slow shear $\langle 1, 1, 0\rangle$ mode.

The photoelastic constants of TeO_2 at 633 nm are

$$p_{11} = .074, \quad p_{12} = .187, \quad p_{13} = .34, \quad p_{31} = .09,$$

$$p_{33} = .24, \quad p_{44} = -.17, \quad p_{66} = -.046$$

For the x-propagating longitudinal mode, the acoustic velocity is

$$v_a = \sqrt{\frac{c_{11}}{\rho}} = 3 \times 10^3 \text{ m/s}$$

For the parallel interaction, $p_{\text{eff}} = p_{11} = .074$ for arbitrary incidence in the yz plane, whereas for the normal interaction the photoelastic constant varies from $p_{12} = .187$ to $p_{31} = .09$, depending on the direction of optic incidence. Because M_2 depends on p_{eff}^2, it is quite important to choose the best interaction geometry. In this case, we choose optic incidence along the z-axis and polarization along the y-axis (the normal interaction involving p_{12}). Then M_2 is

$$M_2 = \frac{n^6 p^2}{\rho\, v_a^3} = 3.0 \times 10^{-14}\ \mathrm{s^3/kg}$$

For the z-propagating longitudinal mode, the optimal configuration involves the perpendicular interaction and $p_{\text{eff}} = .34$. The phase velocity in this case involves the stiffness component c_{33} and is 4.2×10^3 m/s. The FOM for the interaction is 3.5×10^{-14} s^3/kg. In both of these interactions, the optic beam was polarized normal in the xy plane, which required the use of n_o for the index of refraction. Of the two cases considered here, the z-propagating acoustic mode is superior not only because its FOM is larger than that for the x-propagating mode, but also because the higher phase velocity results in a wider Bragg bandwidth. It is a popular interaction geometry at frequencies near 1 GHz.

Finally, for the slow shear, birefringent interaction, the propagation and polarization of the acoustic mode are in the xy plane. Thus, the relevant strain is S_6 and $p_{\text{eff}} = p_{66} = -.046$. As we saw in Chapter 8, the optic incidence is along the z-axis and the polarization is circular (making use of the optical activity of TeO_2). Even though p_{eff} is the smallest of the photoelastic components, the FOM for the interaction is quite large because of the anomalously small phase velocity. As we have seen, this geometry is quite popular at frequencies below 100 MHz. The frequency is limited by the large acoustic attenuation. Substituting values, we determine $M_2 = 7.9 \times 10^{-13}$ s^3/kg. In all cases that we have considered, the FOM of the interaction is an extremely small number. Nevertheless, the intensity of the diffracted light may be quite significant.

9.4 ORTHORHOMBIC INTERACTIONS

The orthorhombic photoelastic matrix contains 12 independent components and has the form:

$$\mathbf{p} = \begin{bmatrix} p_{11} & p_{12} & p_{13} & 0 & 0 & 0 \\ p_{21} & p_{22} & p_{23} & 0 & 0 & 0 \\ p_{31} & p_{32} & p_{33} & 0 & 0 & 0 \\ 0 & 0 & 0 & p_{44} & 0 & 0 \\ 0 & 0 & 0 & 0 & p_{55} & 0 \\ 0 & 0 & 0 & 0 & 0 & p_{66} \end{bmatrix} \tag{9.9}$$

Again, the off-diagonal symmetry of the stiffness matrix reduces the number of components in $\mathbf{c}$ to nine. All six equations of (9.6) contain different photoelastic constants as well as indices of refraction, making the general interaction rather cumbersome.

Lead molybdate is a popular orthorhombic A/O substrate because of its excellent optical properties, relatively low acoustic attenuation, and high FOM. For the $\langle z \rangle$ longitudinal wave, the perturbed index ellipsoid is

$$S_3: \quad x^2\left(\frac{1}{n_1^2} + p_{13}S_3\right) + y^2\left(\frac{1}{n_2^2} + p_{23}S_3\right) + z^2\left(\frac{1}{n_3^2} + p_{33}S_3\right) = 1 \qquad (9.10)$$

Note that in (9.10) we have written the three indices of refraction explicitly. The value of the interaction index depends on the propagation and polarization directions of the incident optic beam and is determined from the index ellipsoid (recall that this symmetry is biaxial and z is not an optic axis). Because there are no cross terms in (9.10), the optic polarization does not flip. A strong diffracted light intensity is achieved for the parallel interaction for which $p_{\text{eff}} = p_{33} = .3$ and $M_2 = 3.6 \times 10^{-14}$ s^3/kg.

9.5 TRIGONAL SYMMETRY

Trigonal symmetry is especially important because it includes $LiNbO_3$. The form of the photoelastic matrix for the classes $3m$, 32, and $\bar{3}m$ (which include $LiNbO_3$ and quartz) has eight independent components. The form of $\mathbf{p}$ is

$$\mathbf{p} = \begin{bmatrix} p_{11} & p_{12} & p_{13} & p_{14} & 0 & 0 \\ p_{12} & p_{11} & p_{13} & -p_{14} & 0 & 0 \\ p_{31} & p_{31} & p_{33} & 0 & 0 & 0 \\ p_{41} & -p_{41} & 0 & p_{44} & 0 & 0 \\ 0 & 0 & 0 & 0 & p_{44} & p_{41} \\ 0 & 0 & 0 & 0 & p_{14} & p_{66} \end{bmatrix}, \; p_{66} = \frac{p_{11} - p_{12}}{2} \qquad (9.11)$$

The terms p_{41} and $p_{42} = -p_{41}$ represent coupling between longitudinal x- and y-polarized acoustic waves (S_1 and S_2) and perturbation terms in the index ellipsoid, which results in polarization flipped interactions (ΔB_4). Likewise, the p_{14} and $p_{24} = -p_{14}$ terms represent shear waves (S_4) that do *not* cause polarization flipped interactions (because they result in perturbations ΔB_1 and ΔB_2). Finally, the terms $p_{56} = p_{41}$ and $p_{65} = p_{14}$ result in additional shear polarization flipped interactions.

One simplification of this symmetry over the orthorhombic system is that it is uniaxial, so there are only two indices n_o and n_e. Because of the complex nature of the interactions, it is helpful to consider each of the principal acoustic waves individually. We write the six equations for the trigonal classes as

$$S_1:\quad x^2\left(\frac{1}{n_o^2} + p_{11}S_1\right) + y^2\left(\frac{1}{n_o^2} + p_{12}S_1\right) + z^2\left(\frac{1}{n_e^2} + p_{31}S_1\right) + 2p_{41}S_1yz = 1$$

$$S_2:\quad x^2\left(\frac{1}{n_o^2} + p_{12}S_2\right) + y^2\left(\frac{1}{n_o^2} + p_{11}S_2\right) + z^2\left(\frac{1}{n_e^2} + p_{31}S_2\right) - 2p_{41}S_2yz = 1$$

$$S_3:\quad x^2\left(\frac{1}{n_o^2} + p_{13}S_3\right) + y^2\left(\frac{1}{n_o^2} + p_{13}S_3\right) + z^2\left(\frac{1}{n_e^2} + p_{33}S_3\right) = 1$$

$$S_4:\quad x^2\left(\frac{1}{n_o^2} + p_{14}S_4\right) + y^2\left(\frac{1}{n_o^2} - p_{14}S_4\right) + \frac{z^2}{n_e^2} + 2p_{44}S_4yz = 1$$

$$S_5:\quad \frac{x^2 + y^2}{n_o^2} + \frac{z^2}{n_e^2} + 2p_{44}S_5xz + 2p_{14}S_5xy = 1$$

$$S_6:\quad \frac{x^2 + y^2}{n_o^2} + \frac{z^2}{n_e^2} + 2p_{41}S_6xz + 2p_{66}S_6xy = 1 \tag{9.12}$$

We first consider S_{11} the x-propagating longitudinal wave with optic polarization parallel to the acoustic beam. This is the ordinary beam because it remains x-polarized as the laser is rotated around the acoustic beam. The photoelastic constant for this interaction geometry is simply p_{11}, and it does not depend on the direction of the optic beam. The normal polarization represents the extraordinary mode, because its index varies from n_e for incidence along the y-axis to n_o for z- or optic-axis incidence. Likewise, the effective photoelastic constant varies with the direction of optic incidence. At y incidence, it is simply p_{31}, and at z incidence it is p_{12}. At an intermediate direction, it may be larger or smaller, depending on the specific photoelastic component values.

Example 9.2. Calculate the effective photoelastic constant for the $\langle x \rangle$ longitudinal propagating wave with the extraordinary (normal) optic beam in the yz plane for $LiNbO_3$. For an A/O device centered at 2 GHz with a 1 GHz bandwidth, calculate the diffracted light efficiency.

Consider the interaction geometry as shown in Figure 9.4. As the optic beam rotates around the x-axis, we rotate the *coordinate* system so that y' corresponds to the incident optic beam and z' corresponds to the polarization direction. The required transformation is given by the orthogonal rotation matrix,

$$\begin{bmatrix} x' \\ y' \\ z' \end{bmatrix} = \begin{bmatrix} 1 & 0 & 0 \\ 0 & \cos\theta & \sin\theta \\ 0 & -\sin\theta & \cos\theta \end{bmatrix} \begin{bmatrix} x \\ y \\ z \end{bmatrix} = \mathbf{R{:}r} \tag{9.13}$$

Because $\mathbf{R}$ is orthogonal, we can immediately solve for y and z in terms of y' and z':

$$\begin{aligned} y &= y' \cos\theta - z' \sin\theta \\ z &= y' \sin\theta + z' \cos\theta \end{aligned} \tag{9.14}$$

Substituting these values into the S_1 equation of (9.12) yields an equation involving the y' and z' coordinates. We need only consider the z'-axis, which corresponds to the required polarization direction. The required effective photoelastic constant is

$$p_{\text{eff}} = p_{12} \sin^2\theta + p_{31} \cos^2\theta - 2p_{41} \sin\theta \cos\theta \tag{9.15}$$

The angles of maximum photoelastic constants are determined by differentiating (9.15) with respect to and setting the result equal to zero:

$$\tan(2\theta) = \frac{2p_{41}}{p_{12} - p_{31}} \tag{9.16}$$

The presence of p_{41} causes the maximum value to lie away from the principal axes. For $LiNbO_3$, the relevant photoelastic components are

$$p_{11} = -.03, \quad p_{12} = .09, \quad p_{31} = .13, \quad p_{41} = -.15$$

Thus the maximum interaction occurs at $\theta = 36.6°$ with a value (from (9.15) of .29. There is a much smaller maximum at $\theta = 127°$.

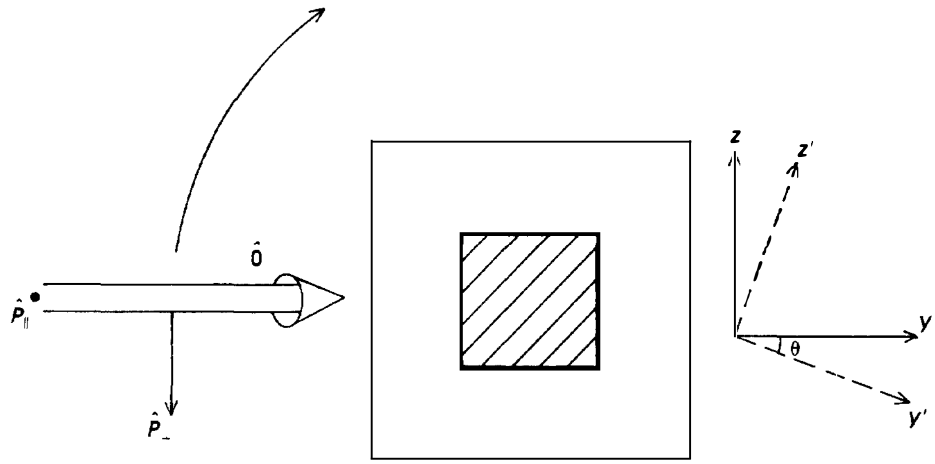

Figure 9.4 Interaction geometry of the $\langle x \rangle$ longitudinal acoustic mode in $LiNbO_3$ (example 9.2). As the optic beam rotates about the acoustic beam, the coordinate system rotates with it.

Note that there are points of zero p_{eff}. An optic beam incident at these directions will not interact with the acoustic wave no matter how much power it possesses. One of these points is very close to $-36°$. If careful attention is not paid to the sign of the crystal axes, a device can easily be fabricated at this angle.

Figure 9.5 shows the variation of photoelastic constant for $LiNbO_3$ as a function of direction and polarization of the incident optic beam. The FOM for the interaction is

$$M_2 = \frac{n^6 p^2}{\rho v_a^3} = 7.86 \times 10^{-15}\ s^3/\text{kg}$$

where $v_a = 6.57 \times 10^3$ m/s is found from the Christoffel equation. For an interaction length of 5 mils at 633 nm and an RF center frequency of 2 GHz, the Bragg bandwidth for this mode is (from (8.8))

$$\text{BW} = \frac{1.8 v_a^2 n}{\lambda_0 f L} = 1.1\ \text{GHz}$$

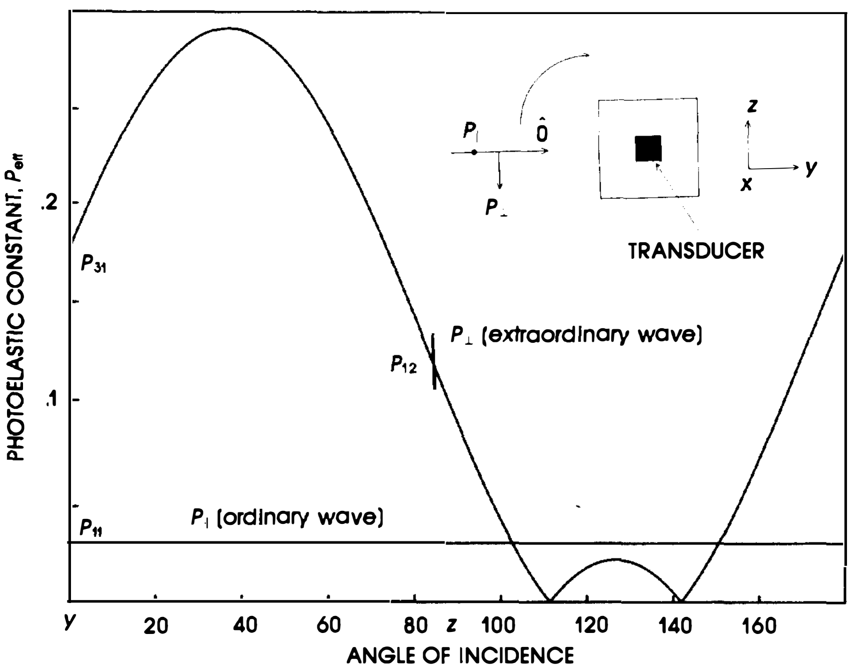

Figure 9.5 Results of the calculation of Example 9.2 showing the effective photoelastic constant dependance on optic incidence. θ is measured from the y-axis. Note that for the parallel interaction, p_{eff} is constant as in the cubic and isotropic systems.

The diffraction light efficiency is given by (8.3) (let $H = L$):

$$\frac{I_d}{I_i} = \frac{\pi^2 L}{2\lambda_0^2 H} M_2 P_a = 9.7 \times 10^{-2} P_a$$

The diffracted light power is thus nearly 10% of the incident light power for 1 W of *acoustic* power. If the conversion of energy from RF to acoustic results in a 6-dB conversion loss, the diffracted light will be approximately 2% of the incident light for 1 W of RF. At a 2-GHz center frequency with a 36 degree $\langle y \rangle$ longitudinal transducer, we can expect a bandwidth of about 1 GHz, so the acoustic and Bragg bands are well matched in this region. The radiation impedance is (because there is a good acoustic match between transducer and substrate) $\hat{R}_a = 7\ \Omega$.

Finally, the beam divergence angle plane normal to the plane of incidence (i.e., due to H) is less than 2°. Resolutions of 1 MHz or less have easily been achieved (a 1-MHz resolution requires a τ of 1 μs or an acoustic path length of 6.6 mm). This device design has been commercially available since about 1975. It has an excellent combination of characteristics at HeNe wavelengths, but suffers from relatively poor efficiency at laser diode wavelengths and has since been supplanted by newer designs and materials.

Returning to the x-propagating longitudinal mode (S_1) in (9.10), we see that there is a polarization flipped interaction involving the photoelastic constant p_{41}. The "flip" is between y- and z-polarizations, so the optic beam is required to be incident along the x-axis. This interaction is thus a *collinear* interaction. It is also birefringent because the polarization flips between the z (ordinary) and y (extraordinary) modes. The critical frequency for the interaction is given by (7.111) with

$$v_a = 6.57 \times 10^3 \text{ m/s} \quad f_s' = 6.6 \text{ GHz at } 633 \text{ nm}$$

$$f_s' = 4.7 \text{ GHz at } 830 \text{ nm}$$

Because of the extremely high critical frequency for the interaction, it is not particularly useful.

For the y-polarized longitudinal acoustic wave (S_2), the equation for the perturbed index is quite similar to S_1. The acoustic velocity for this mode is 5% higher than that for the x-propagating mode, and thus the Bragg bandwidth is somewhat larger while the diffraction efficiency is about 15% lower. Isotropic interactions based on this wave have not been exploited. As in the previous case, the polarization flipped interaction involving p_{41} requires an x-propagating optic beam; this interaction is not collinear and is thus potentially useful for wideband spectrum analysis. The critical frequency is 6.9 GHz at 633 nm and about 5 GHz at 830 nm. A device based on this interaction has been reported [8].

For the z-propagating longitudinal mode (S_3), the perturbed index ellipsoid is quite similar to the cubic symmetry. There are no polarization flipped interactions, and the isotropic interactions are not particularly robust. This is due in part because of the very high acoustic velocity for this mode (7.2×10^3 m/s). For an optic beam incident in the xy plane polarized parallel to the acoustic polarization, the effective photoelastic constant is p_{33}; for the perpendicular polarization, it is p_{13} (independent of the optic beam direction).

For the S_4 acoustic wave (y-propagating, z-polarized) interacting with an x-incident optic beam polarized along y, an isotropic interaction exists with $p_{\text{eff}} = p_{14}$. This same beam also possesses a polarization flipped birefringent interaction between y- and z-polarizations with effective constant of $2p_{44}$. Thus, for frequencies above the minimum value for the birefringent interaction, the diffracted light will consist of both components. With a polarizer, it is possible to separate these components and determine the fraction of diffracted light for each interaction. For an optic beam incident along y and polarized along x, $p_{\text{eff}} = p_{14}$, but in this case there is only one (nonflipped) interaction.

The S_5 shear wave has two possible polarization flipped interactions involving p_{44} and p_{14}. For x-incident light polarized along either y or z, there is no interaction because the polarization that is normal to x does not couple with either perturbation terms. For y incidence (polarized along either x or z), there is a birefringent interaction with p_{44}, whereas for z incidence there is an isotropic interaction that is polarization flipped between x and y. These same results are valid for S_6, in which the perturbed index ellipsoid has the same form as for S_5.

9.6 ARBITRARY ACOUSTIC DIRECTIONS

We have described the possible interactions in Section 9.5 for the principal longitudinal and shear modes. Although more complex, the photoelastic constant can usually be found by inspection (except for the $\langle x \rangle$ longitudinal mode in $LiNbO_3$) in much the same way that the stiffness constants were determined for acoustic propagation along the principal axes. If the acoustic propagation direction does not coincide with one of the principal axis, the description of the interaction requires the admixture of at least two of the photoelastic equations for the perturbed index ellipsoid. This increases the possible interaction geometries as well as the possibilities for improved performance. Like the calculation of acoustic phase velocities, however, the determination of the interaction parameters will probably involve computer-aided solutions. The exception to this rule is the isotropic case, for which all directions are equivalent.

We consider the case of a longitudinal wave in a cubic class $\bar{4}3m$ propagating in the $\langle 1, 1, 0 \rangle$ direction. The strain is given by (1.86):

$$\mathbf{S} = \nabla_s \mathbf{u}$$

where for a plane wave the gradient operator is the 6×3 matrix given by (1.85). Because the $\langle 1, 1, 0 \rangle$ longitudinal wave is pure, the polarization (particle) displacement) is also $\langle 1, 1, 0 \rangle$ directed. The strain in this case is

$$\mathbf{S} = \frac{1}{2} \begin{bmatrix} 1 & 0 & 0 \\ 0 & 1 & 0 \\ 0 & 0 & 0 \\ 0 & 0 & 0 \\ 0 & 0 & 0 \\ 1 & 1 & 0 \end{bmatrix} \begin{bmatrix} 1 \\ 1 \\ 0 \end{bmatrix} = \begin{bmatrix} .5 \\ .5 \\ 0 \\ 0 \\ 0 \\ 1 \end{bmatrix}$$

The perturbation is given by (9.3):

$$\Delta\mathbf{B} = \mathbf{p}{:}\mathbf{S} = \frac{1}{2}\begin{bmatrix} p_{11} + p_{12} \\ p_{11} + p_{12} \\ 2p_{12} \\ 0 \\ 0 \\ 2p_{44} \end{bmatrix}$$

The perturbed index ellipsoid is thus

$$x^2\left(\frac{1}{n_o^2} + \frac{p_{11} + p_{12}}{2} S\right) + y^2\left(\frac{1}{n_o^2} + \frac{p_{11} + p_{12}}{2} S\right) + 2p_{44}Sxy + z^2\left(\frac{1}{n_o^2} + p_{12}S\right) = 1 \tag{9.17}$$

The interaction geometry is shown in Figure 9.6.

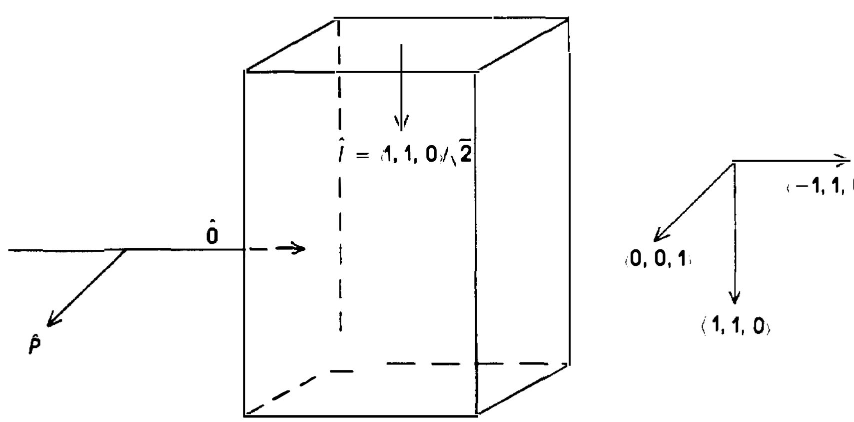

Figure 9.6 Determination of p_{eff} for "off-axis" acoustic beam. The case considered in this figure is relatively simple because $\hat{\mathbf{l}}$ is a symmetry direction in the cubic system.

The simplest case is that of an optic beam incident along the $\langle -1, 1, 0\rangle$ and z-polarized. From (9.17), the effective photoelastic constant is just p_{12}. If we consider only the perturbation, then the remaining part (excluding the z term) of (9.17) has the form:

$$Ax^2 + Ay^2 + 2Cxy = 1 \tag{9.18}$$

where

$$A = \frac{p_{11} + p_{12}}{2} \text{ and } C = p_{44}$$

Equation (9.18) represents an ellipse in the *xy plane* rotated by 45°. This is the form of a polarization flipped interaction only if the incident optic beam is polarized along the x-axis. In the present case, it is directed along $\langle 1, 1, 0\rangle$, which is parallel to the acoustic polarization and 45° from the x-axis. We can use the 45° rotation matrix about the z-axis (7.57) to transform the xy (crystal axis) system into a set of coordinates valid for the particular directions of acoustic and optic beams in the interaction. The approach is identical to that of Example 9.2, even though the geometry is somewhat more complex. Solving for x', y' in terms of x, y, we have

$$x = \frac{x' - y'}{\sqrt{2}}, \; y = \frac{x' + y'}{\sqrt{2}}$$

where the x'-axis represents the $\langle 1, 1, 0\rangle$ direction and the y'-axis represents the $\langle 1, -1, 0\rangle = \langle -1, 1, 0\rangle$ direction. Substituting the xy system in terms of x', y' into (9.18), we immediately get

$$(A + C)x'^2 + (A - C)y'^2 = 1 \tag{9.19}$$

Thus for an optic beam polarized along $\langle 1, 1, 0\rangle$, the effective photoelastic constant is

$$p_{\text{eff}} = A + C = \frac{p_{11} + p_{12}}{2} + p_{44} \tag{9.20}$$

This is the case considered earlier in which the optic and acoustic polarizations (for a longitudinal wave) are parallel. For optic polarization along $\langle -1, 1, 0\rangle$, the effective photoelastic constant is

$$p_{\text{eff}} = A - C = \frac{p_{11} + p_{12}}{2} - p_{44} \tag{9.21}$$

This is the case in which the optic polarization and acoustic polarizations are normal, and the optic beam is incident along the z-axis. These results are summarized in Figure 9.7.

We are tempted to seek a polarization flipped interaction from the form of (9.18). Such an interaction occurs for optic polarizations along the x and y directions but not along the x' or y' directions. This interaction

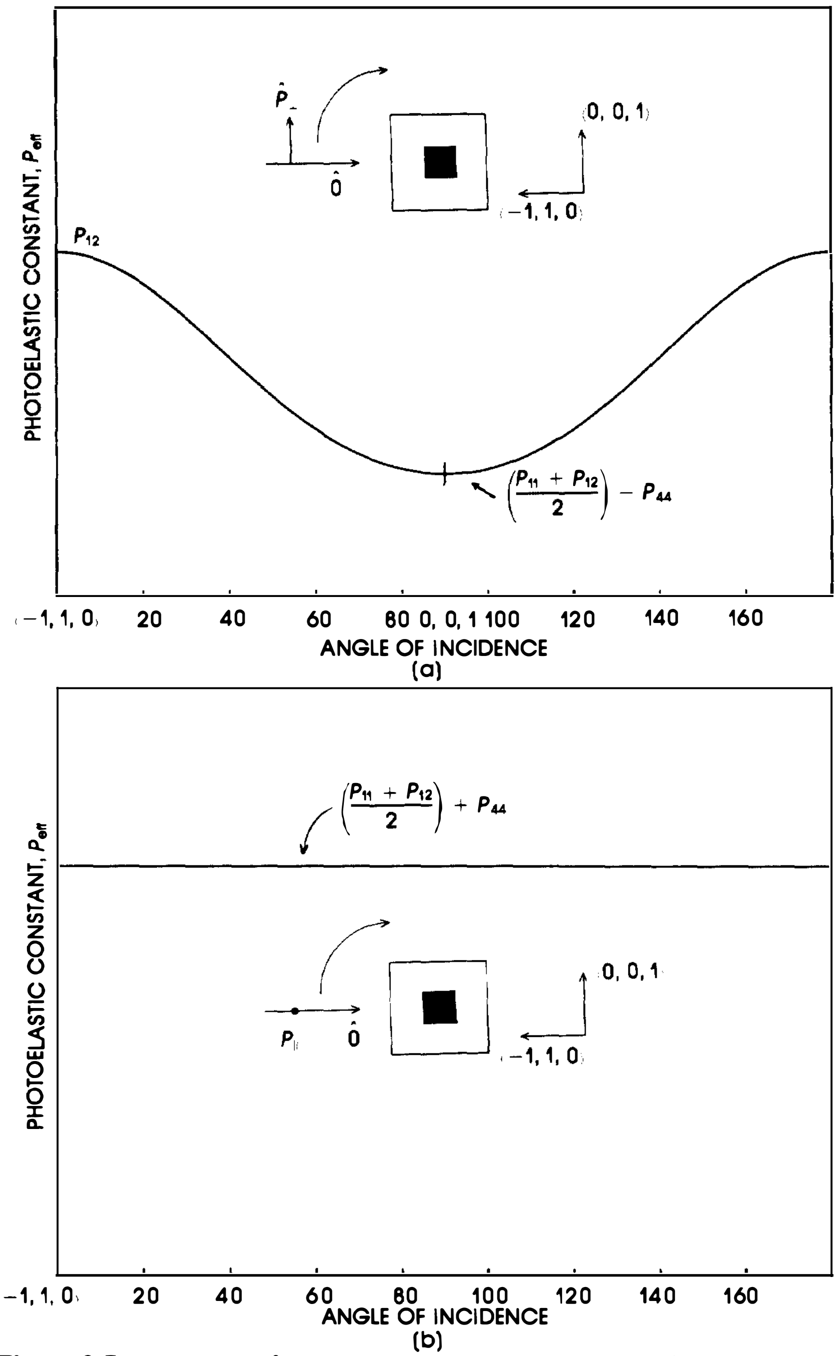

Figure 9.7 Variation of p_{eff} with optic beam incidence for the ⟨1, 1, 0⟩ acoustic beam for the (a) perpendicular and (b) parallel interactions. $\theta = 0$ corresponds to the ⟨−1, 1, 0⟩ direction.

can be realized, however, by simply rotating the laser (if it is linearly polarized) by 45°.

9.7 COMPUTER-AIDED ANALYSIS OF COMPLEX INTERACTION GEOMETRIES

In principle, any acoustic wave can be handled by searching for axes in which the optic polarization is either parallel or normal to the acoustic polarization. For an arbitrary acoustic propagation direction, this procedure can be quite cumbersome in practice. In this section, we develop a straightforward technique to determine the effective photoelastic constants for given acoustic propagation and polarization directions. As before, we assume that these constants are known from solving the Christoffel equation.

We first transform the crystal axes system into a coordinate system that represents the acoustic propagation direction and an initial direction of optic incidence. This transformation is defined by the matrix $\mathbf{R}_1$:

$$\mathbf{R}_1 = \begin{bmatrix} l_x & l_y & l_z \\ O_1 & O_2 & O_3 \\ N_1 & N_2 & N_3 \end{bmatrix} \tag{9.22}$$

where $\hat{\mathbf{l}} = (l_x, l_y, l_z)$ represents the acoustic propagation direction, $\hat{\mathbf{O}} = (O_1, O_2, O_3)$ is the normalized optic beam direction, and $\hat{\mathbf{N}} = (\mathrm{N}_1, \mathrm{N}_2, \mathrm{N}_3)$ is a vector perpendicular to both:

$$\hat{\mathbf{N}} = \hat{\mathbf{l}} \times \hat{\mathbf{O}}$$

For optically isotropic symmetries, $\hat{\mathbf{O}}$ can be defined arbitrarily. For anisotropic crystals, it is usually convenient to define $\hat{\mathbf{O}}$ with respect to the optic axes. The matrix $\mathbf{R}_1$ is a generalization of the 45° rotation considered in the previous section. As we have already seen, there are two operations of interest:

1. Rotation of the optic beam around the acoustic beam while holding the polarization direction fixed (with respect to the optic beam);
2. Rotation of the optic polarization while holding the optic direction of incidence fixed.

The first operation aids in finding the optimal crystal cut for a given acoustic wave. The second operation is of interest because, although the polarization direction can be changed (by simply rotating the laser), optimal device operation requires that the polarization direction be properly set. The optic incidence direction is rotated around the acoustic beam by using the matrix:

$$\mathbf{R}_2 = \begin{bmatrix} 1 & 0 & 0 \\ 0 & \cos\theta & \sin\theta \\ 0 & -\sin\theta & \cos\theta \end{bmatrix} \tag{9.23}$$

where θ is the rotation angle. Equation (9.23) follows from the fact that the acoustic beam is represented as the "x"-axis in the transformation $\mathbf{R}_1$. Equation (9.23) represents a simple rotation around the x (acoustic) axis. Likewise, the optic polarization rotation is represented by the matrix (which is a rotation around the $\hat{\mathbf{O}}$ axis):

$$\mathbf{R}_3 = \begin{bmatrix} \cos\phi & 0 & \sin\phi \\ 0 & 1 & 0 \\ -\sin\phi & 0 & \cos\phi \end{bmatrix} \tag{9.24}$$

In practice, either one or the other of the matrices $\mathbf{R}_2$ or $\mathbf{R}_3$, but not both, can be applied for a given situation. From (9.24), it is clear that the first and third rows of $\mathbf{R}_3$ represent optic polarization directions because they are vectors normal to $\hat{\mathbf{O}}$. If the angle ϕ is constant, the polarizations are fixed (in the Cartesian system). By varying ϕ, we obtain curves that show the dependence of the effective photoelastic constant with optic polarization. For an isotropic interaction, it is convenient to define them as either parallel or normal to the acoustic polarization, whereas for a birefringent interaction they are best defined as the polarizations of the ordinary and extraordinary modes (and thus represent explicitly the incident and diffracted optic beams). The axes of the two polarizations with respect to the original Cartesian coordinates are given by the matrix product,

$$\mathbf{R} = \mathbf{R}_3{:}\mathbf{R}_2{:}\mathbf{R}_1 \tag{9.25}$$

Writing (9.25) explicitly; we have

$$\begin{bmatrix} x' \\ y' \\ z' \end{bmatrix} = \begin{bmatrix} \mathbf{R} \end{bmatrix} \begin{bmatrix} x \\ y \\ z \end{bmatrix} \tag{9.26}$$

where the primed coordinates (x', z') are the polarization axes, y' is the direction of optic incidence, and the unprimed coordinates x, y, and z represent the (original) Cartesian system.

The perturbed index ellipsoid, as represented by equations of the form (9.6) or (9.12), is written in terms of the original Cartesian system. For a single acoustic wave (not necessarily along a principle axis), it therefore has the form (in the original crystal axis system):

$$Ax^2 + By^2 + Cz^2 + 2Dyz + 2Exz + 2Fxy = 1 \tag{9.27}$$

As before, the unperturbed portion is contained in the first three terms (if we exclude the monoclinic and triclinic symmetries), whereas the perturbation portion can exist in all six terms. The original axes are written in terms of the polarization axes by inverting **R**. Equation (9.26) becomes

$$\begin{bmatrix} x \\ y \\ z \end{bmatrix} = \begin{bmatrix} \mathbf{R}^{-1} \end{bmatrix} \begin{bmatrix} x' \\ y' \\ z' \end{bmatrix} \tag{9.28}$$

To determine the effective photoelastic constant from (9.27), we recall that there are only three possible types of interactions:

1. A nonflipped interaction between an acoustic wave (which may be longitudinal or shear, for trigonal symmetry only) and an optic beam with a specified polarization;
2. A nonflipped interaction between an acoustic wave (longitudinal or shear) and an optic beam polarized with an orthogonal polarization. For cubic symmetry, we generally choose the optic polarizations (which are the first and third rows of $\mathbf{R}_3$) to be parallel and normal to the acoustic wave;
3. A polarization flipped interaction between a longitudinal or shear acoustic wave in which the polarization of the optic beams flips between the first and third rows of $\mathbf{R}_3$. This interaction may be isotropic or birefringent. If it is birefringent, it is clear that the two polarizations correspond to the ordinary and extraordinary modes.

For the parallel interaction, we choose the top row of $\mathbf{R}_3$ to be the desired optic polarization (the choice of top or bottom row is arbitrary). We seek those terms in (9.27) that contain the factors $(x')^2$. Indeed, the sum of all possible such terms determines the effective photoelastic constant and is independent of the optic beam direction. The perturbed index ellipsoid will have the form:

$$(x')^2 \left[\frac{1}{n_o^2} + p_{\text{eff}} S'\right] + (\text{all other terms}) = 1 \tag{9.29}$$

where S' is the given acoustic strain. Using (9.27) and (9.28), we obtain the effective photoelastic constant:

$$p_{\text{eff}} = A(R_{11}^{-1})^2 + B(R_{21}^{-1})^2 + C(R_{31}^{-1})^2 + 2DR_{21}^{-1}R_{31}^{-1} + 2ER_{11}^{-1}R_{31}^{-1} + 2FR_{11}^{-1}R_{21}^{-1} \tag{9.30}$$

By varying the angle θ in matrix $\mathbf{R}_2$, we obtain a curve of p_{eff} *versus* incident optic beam direction. Because the interaction is determined by the orientation of the optic and acoustic polarizations, this curve is usually a constant value, as we saw in Figures 9.2(a) and 9.7(b).

In the interaction between the longitudinal acoustic wave and the normally polarized optic beam, we choose the bottom row of $\mathbf{R}_3$ as the desired optic polarization and collect all terms in (9.27) containing $(z')^2$. The effective photoelastic constant for this interaction is

$$p_{\text{eff}} = A(R_{13}^{-1})^2 + B(R_{23}^{-1})^2 + C(R_{33}^{-1})^2 + 2DR_{23}^{-1}R_{33}^{-1} + 2ER_{13}^{-1}R_{33}^{-1} + 2FR_{13}^{-1}R_{23}^{-1} \tag{9.31}$$

Because the orientation of the acoustic and optic polarizations changes as the optic beam direction varies, p_{eff} will vary with θ as shown in Figures 9.5 and 9.7(a).

Finally, for the polarization flipped interaction, p_{eff} is given by all terms that contain the factor $(x'z')$:

$$\begin{aligned} p_{\text{eff}} = {} & 2AR_{11}^{-1}R_{13}^{-1} + 2BR_{21}^{-1}R_{23}^{-1} + 2CR_{31}^{-1}R_{33}^{-1} \\ & + D(R_{21}^{-1}R_{33}^{-1} + E(R_{11}^{-1}R_{33}^{-1} + R_{31}^{-1}R_{13}^{-1}) \\ & F(R_{11}^{-1}R_{23}^{-1} + R_{21}^{-1}R_{13}^{-1}) \end{aligned} \tag{9.32}$$

Figure 9.8 shows the computer program that calculates p_{eff}, for arbitrary directions of the acoustic wave. The program uses the transformation matrices developed in this section, but each geometry must be considered individually. The input data consist of the polarization direction of the acoustic wave and the photoelastic matrix. Because in practice only symmetry directions are used, this vector can be determined by inspection. For an unusual case, it would be determined by solving the Christoffel equation and substituting the eigenvector explicitly.

Example 9.3. We reconsider the ⟨1, 1, 0⟩ longitudinal wave propagating in a cubic crystal. $\mathbf{R}_1$ is given by (9.22):

$$\mathbf{R}_1 = \begin{bmatrix} 1/\sqrt{2} & 1/\sqrt{2} & 0 \\ -1/\sqrt{2} & 1/\sqrt{2} & 0 \\ 0 & 0 & 1 \end{bmatrix} \begin{array}{l} \leftarrow \text{acoustic direction} \\ \leftarrow \text{optic beam direction } (\theta = 0) \\ \leftarrow \text{cross product of first two rows} \end{array}$$

The initial optic beam direction is arbitrary (we could have chosen any direction normal to ⟨1, 1, 0⟩).

```
1000  OPTION BASE 1
1030  LIBRARY "GRAPHLIB"
1060  SET MODE "HIRES"
1090  SET COLOR 10
1120  DIM U(3,1) !ACOUSTIC POLARIZATION
1150  DIM ST61(6,1) !STRAIN MATRIX
1180  DIM P66(6,6) !PHOTOELASTIC MATRIX
1210  DIM L13(1,3) !DIRECTION OF ACOUSTIC PROPAGATION
1240  INPUT PROMPT "DIRECTION OF PROPAGATION:":L13(1,1),L13(1,2),L13(1,3)
1270  LET LN=(L13(1,1)^2+L13(1,2)^2+L13(1,3)^2)^.5
1300  LET L13(1,1)=L13(1,1)/LN
1330  LET L13(1,2)=L13(1,2)/LN
1360  LET L13(1,3)=L13(1,3)/LN
1390  DIM DELB(6,1),INVR(3,3)
1420  DIM R1(3,3)
1450  DIM R2(3,3)
1480  DIM R3(3,3)
1510  DIM R4(3,3),R5(3,3)
1540  DIM L36(3,6),L63(6,3)
1570  MAT READ P66(6,6) !READ IN THE PHOTOELASTIC MATRIX FOR GAP
1600  DATA -.151,-.082,-.082,0,0,0
1630  DATA -.082,-.151,-.082,0,0,0
1660  DATA -.082,-.082,-.151,0,0,0
1690  DATA 0,0,0,-.074,0,0
1720  DATA 0,0,0,0,-.074,0
1750  DATA 0,0,0,0,0,-.074
1780  ! THIS IS THE DIVERGENCE MATRIX OPERATOR
1810  LET L36(1,1)=L13(1,1)
1840  LET L36(2,2)=L13(1,2)
1870  LET L36(3,3)=L13(1,3)
1900  LET L36(1,5)=L13(1,3)
1930  LET L36(1,6)=L13(1,2)
1960  LET L36(2,4)=L13(1,3)
1990  LET L36(2,6)=L13(1,1)
2020  LET L36(3,4)=L13(1,2)
2050  LET L36(3,5)=L13(1,1)
2080  !TRANSPOSE OF L36 IS THE GRADIENT MATRIX OPERATOR
2110  MAT L63 = TRN(L36)
2140  INPUT PROMPT "POLARIZATION DIRECTION:": U(1,1),U(2,1),U(3,1)
2170  LET UN=(U(1,1)^2+U(2,1)^2+U(3,1)^2)^.5
2200  LET U(1,1)=U(1,1)/UN
2230  LET U(2,1)=U(2,1)/UN
2260  LET U(3,1)=U(3,1)/UN
2290  MAT PRINT L63
2320  MAT ST61=L63*U  !STRAIN IS THE GRADIENT OF DISPLACEMENT (EQ.1.86)
2350  PRINT "ST",ST61(1,1),ST61(2,1),ST61(3,1),ST61(4,1),ST61(5,1),ST61(6,1)
2380  MAT DELB=P66*ST61 !PERTURBATION TO THE INDEX ELLIPSOID
2410  PRINT "DELB",DELB(1,1),DELB(2,1),DELB(3,1),DELB(4,1),DELB(5,1),DELB(6,1)
2440  LET FLIP$="N"
2470  INPUT PROMPT "DO YOU WISH A POLARIZATION FLIP?:": FLIP$
2500  LET N1=(L13(1,1)^2+L13(1,2)^2)^.5
2530  LET  R1(1,1)=L13(1,1)
2560  LET  R1(1,2)=L13(1,2)
2590  LET  R1(1,3)=L13(1,3)
2620  !FIRST ROW OF R1(3,3) IS THE ACOUSTIC PROPAGATION DIRECTION
2650  LET  R1(2,1)=-L13(1,2)/N1
2680  LET  R1(2,2)=L13(1,1)/N1
2710  LET  R1(2,3)=0
2740  !SECOND ROW IS THE INITIAL OPTIC DIRECTION
2770  !HERE THE INITIAL OPTIC DIRECTION IS NORMAL TO THE Z AXIS
```

Figure 9.8 Computer program listing for calculation of p_{eff} for arbitrary acoustic propagation direction.

```
2800  LET  R1(3,1)=-L13(1,1)*L13(1,3)/N1
2830  LET  R1(3,2)=-L13(1,2)*L13(1,3)/N1
2860  LET  R1(3,3)=N1
2890  !THIRD ROW IS THE CROSS PRODUCT OF ROWS 1 AND 2
2920  OPEN #1:SCREEN  .3,.9,.20,.9
2950  SET WINDOW 0,PI,0,.25
2980  SET MODE "HIRES"
3010  CALL AXES
3040  CALL TICKS(PI/6,.05)
3070  CALL FRAME
3100  FOR PHI=0 TO PI STEP PI/180
3130  !IN THIS CASE THE OPTIC BEAM ROTATES AROUND THE ACOUSTIC WAVE
3160  !THE OPTIC POLARIZATION DIRECTION IS FIXED (R3(3,3)=I)
3190  LET R2(1,1)=1
3220  LET R2(1,2)=0
3250  LET R2(1,3)=0
3280  LET R2(2,1)=0
3310  LET R2(2,2)=COS(PHI)
3340  LET R2(2,3)=SIN(PHI)
3370  LET R2(3,1)=0
3400  LET R2(3,2)=-SIN(PHI)
3430  LET R2(3,3)=COS(PHI)
3460  LET R3(1,1)=1
3490  LET R3(1,2)=0
3520  LET R3(1,3)=0
3550  LET R3(2,1)=0
3580  LET R3(2,2)=1
3610  LET R3(2,3)=0
3640  LET R3(3,1)=0
3670  LET R3(3,2)=0
3700  LET R3(3,3)=1
3730  MAT R4=R2*R1
3760  MAT R5=R3*R4
3790  MAT INVR=INV(R5)
3820  IF FLIP$="Y" THEN GOTO 4060
3850  !IN THIS EXAMPLE THE ACOUSTIC AND OPTIC POLARIZATION ARE PARALLEL (9.30)
3880  !FOR THE NORMAL CASE (9.31) CHANGE INVR(I,1) TO INVR(I,3)
3910 LET PSUM=DELB(1,1)*INVR(1,1)^2+DELB(2,1)*INVR(2,1)^2+DELB(3,1)*INVR(3,1)^2
3940  LET PSUM=PSUM+2*DELB(4,1)*INVR(2,1)*INVR(3,1)
3970  LET PSUM=PSUM+2*DELB(5,1)*INVR(1,1)*INVR(3,1)
4000  LET PSUM=PSUM+2*DELB(6,1)*INVR(1,1)*INVR(2,1)
4030  GOTO 4240
4060  LET PSUM=2*DELB(1,1)*INVR(1,1)*INVR(1,3)
4090  LET PSUM=PSUM+2*DELB(2,1)*INVR(2,1)*INVR(2,3)
4120  LET PSUM=PSUM+2*DELB(3,1)*INVR(3,1)*INVR(3,3)
4150  LET PSUM=PSUM+DELB(4,1)*(INVR(2,1)*INVR(3,3)+INVR(3,1)*INVR(2,3))
4180  LET PSUM=PSUM+DELB(5,1)*(INVR(1,1)*INVR(3,3)+INVR(3,1)*INVR(1,3))
4210  LET PSUM=PSUM+DELB(6,1)*(INVR(1,1)*INVR(2,3)+INVR(2,1)*INVR(1,3))
4240  LET PEFF=ABS(PSUM)
4270  !PRINT PHI*180/PI,PEFF
4300  PLOT PHI,PEFF;
4330  NEXT PHI
4360  OPEN #2:SCREEN 0,.28,0,1
4390  SET WINDOW -1,1,-1,1
4420  SET CURSOR 13,21
4450  PRINT ".1"
4480  OPEN #3:SCREEN .3,1,0,.1934
4510  SET WINDOW -1,1,-1,1
4540  SET CURSOR 1,1
4570  PRINT "0"
```

```
4600  SET CURSOR 1,16
4630  PRINT "60"
4660  SET CURSOR 1,32
4690  PRINT "120"
4720  SET CURSOR 1,48
4750  PRINT "180"
4780  SET CURSOR 3,20
4810  PRINT "ANGLE"
4840  OPEN #4:SCREEN .3,1,.91,1
4870  SET WINDOW -1,1,-1,1
4900  SET CURSOR 1,18
4930  PRINT "PHOTOELASTIC CONSTANT"
4960  END
```

Rotation about the Acoustic Direction

$\mathbf{R}_3$ is the identity matrix, and $\mathbf{R}_2$ is given by (9.23). Equation (9.25) becomes

$$\mathbf{R} = \mathbf{R}_3{:}\mathbf{R}_2{:}\mathbf{R}_1 = \mathbf{I}{:}\mathbf{R}_2{:}\mathbf{R}_1$$

$$= \begin{bmatrix} 1/\sqrt{2} & 1/\sqrt{2} & 0 \\ -\cos\theta/\sqrt{2} & \cos\theta/\sqrt{2} & \sin\theta/\sqrt{2} \\ \sin\theta/\sqrt{2} & -\sin\theta/\sqrt{2} & \cos\theta/\sqrt{2} \end{bmatrix} \begin{array}{l} \leftarrow \text{parallel polarization} \\ \\ \leftarrow \text{normal polarization} \end{array}$$

Notice that the parallel polarization does not depend on the direction of optic incidence. At $\theta = 0$, the normal polarization is (0, 0, 1), and at $\theta = \pi/2$ it is (1, -1, 0), as shown in Figure 9.7. For the polarization rotation, we have

$$\mathbf{R} = \mathbf{R}_3{:}\mathbf{I}{:}\mathbf{R}_1$$

$$= \begin{bmatrix} \cos\phi/\sqrt{2} & \cos\phi/\sqrt{2} & \sin\phi \\ -1/\sqrt{2} & 1/\sqrt{2} & 0 \\ -\sin\phi/\sqrt{2} & -\sin\phi/\sqrt{2} & \cos\phi \end{bmatrix}$$

At $\phi = 0$, the first and third rows are parallel and normal to $\hat{\mathbf{I}}$; but at $\phi = \pi/2$, the first row is (0, 0, 1) (normal), and the third row is (-1, -1, 0) (parallel). The polarization directions can be fixed relative to $\hat{\mathbf{O}}$ by fixing the angle ϕ.

Because the matrix **R** is orthogonal (it is the product of orthogonal matrices), we immediately have:

$$\mathbf{R}^{-1} = \tilde{\mathbf{R}}$$

At $\theta = \phi = 0$,

$$\mathbf{R}^{-1} = \begin{bmatrix} 1/\sqrt{2} & -1/\sqrt{2} & 0 \\ 1/\sqrt{2} & 1/\sqrt{2} & 0 \\ 0 & 0 & 1 \end{bmatrix}$$

Finally, using (9.30), we get

$$p_{\text{eff}} = \frac{p_{11} + p_{12}}{2} + p_{44} \text{ (for parallel polarization)}$$

and from (9.31),

$$p_{\text{eff}} = \frac{p_{11} + p_{12}}{2} - p_{44} \text{ (for normal polarization)}$$

in agreement with (9.20) and (9.21). Figure 9.9 shows the variation in p_{eff} for the $\langle 1, 0, 0 \rangle$, $\langle 1, 1, 0 \rangle$, and $\langle 1, 1, 1 \rangle$ longitudinal acoustic waves for GaAs when acoustic and optic polarizations are parallel. By optimizing the acoustic mode direction, we see clearly that a dramatic performance advantage can be achieved.

Figure 9.10 shows p_{eff} for the same modes as the polarization angle is varied, and Figure 9.11 shows the variation in p_{eff} with polarization angle for the polarization flipped interaction. Note that the polarization flipped interaction is optimized for a 45° rotation angle and is quite weak compared with the nonflipped.

Example 9.4. Performance of .5-GHz GaP Bragg cell. We now consider the performance of a popular device in A/O spectrum analysis for electronic support measures (ESM) applications. The resolution requirement is about 20 MHz (or 50 ns), so H can be made as small as possible consistent with fabrication constraints. The acoustic wave is longitudinal, the center frequency is 1 GHz, and the optic wavelength is .83 μm. The radiation resistance and Bragg bandwidth place constraints on the transducer length. The velocities of the three modes considered in this section and their corresponding L values (from 8.8)) for a bandwidth of .5 GHz are

$$= 5.85 \times 10^3 \text{ m/s} \rightarrow L = 500\ \mu\text{m (20 mils)}$$

$$= 6.45 \times 10^3 \text{ m/s} \rightarrow L = 600\ \mu\text{m (23 mils)}$$

$$6.65 \times 10^3 \text{ m/s} \rightarrow L = 630\ \mu\text{m (25 mils)}$$

For H, we choose 75 μm (3 mils). The area in each case is consistent with a radiation resistance of about 8 to 10 Ω. The photoelastic constants

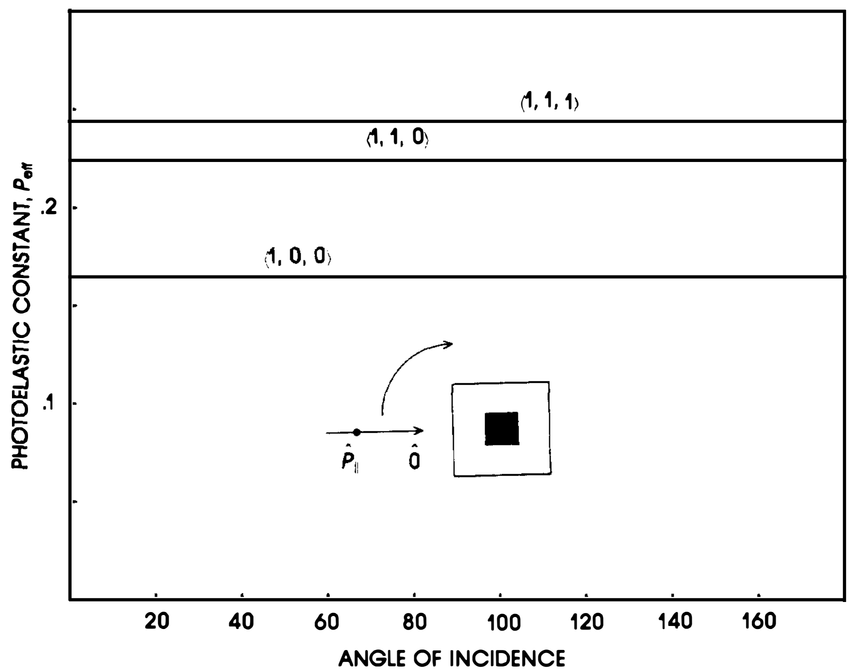

Figure 9.9 Variation of p_{eff} for the parallel interaction for the longitudinal ⟨1, 0, 0⟩, ⟨1, 1, 0⟩, and ⟨1, 1, 1⟩ acoustic modes of GaAs with optic beam incidence. Calculations were performed by using the listing in Figure 9.8.

for the parallel interaction are given by (9.30). Using GaP values, we find for the figures of merit,

$$M_2 = \begin{cases} 3.5 \times 10^{-14} & \langle 1, 0, 0 \rangle \\ 4.2 \times 10^{-14} & \langle 1, 1, 0 \rangle \\ 4.4 \times 10^{-14} & \langle 1, 1, 1 \rangle \end{cases}$$

Substituting the relevant values into (8.3) for the ⟨1, 1, 1⟩ modes, we have

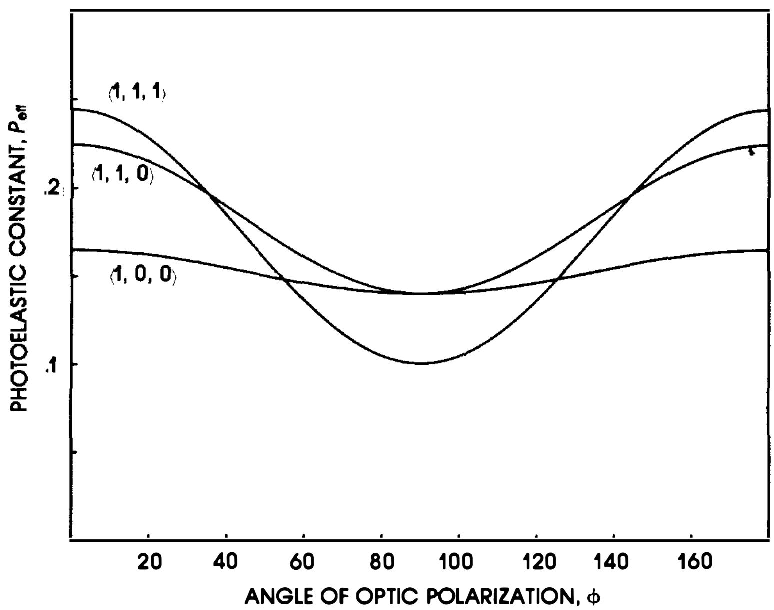

Figure 9.10 Variation of p_{eff} for ⟨1, 0, 0⟩, ⟨1, 1, 0⟩, and ⟨1, 1, 1⟩ acoustic modes of GaAs with optic polarization. $\phi = 0$ corresponds to the parallel direction, and $\phi = 90°$ corresponds to the normal polarization.

$$\frac{I_d}{I_i} = \frac{\pi^2}{2\lambda_0^2}\left(\frac{L}{H}\right)M_2 P_a = 2.24 P_a$$

Thus for 100 mW acoustic power the device will deflect about 22% of the incident radiation (or about 220% per W). Including the RF to acoustic conversion loss, we conclude that the device as designed should have an efficiency of close to 50% per RF watt. At .633 μm, the corresponding efficiency would be about 100%/W. This is consistent with devices fabricated thus far. As we noted in Chapter 8, use of multiple acoustic waves and phase array techniques provide performance enhancements of up to 300%.

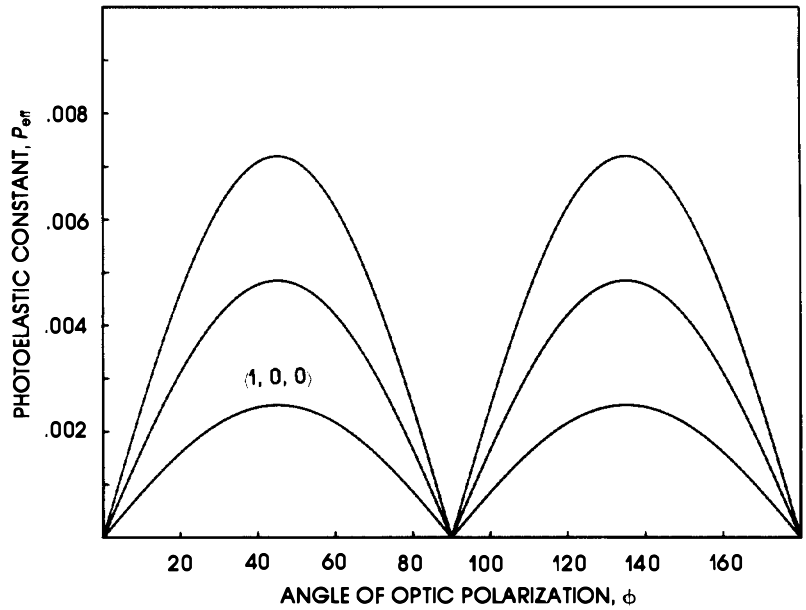

Figure 9.11 Variation of p_{eff} for longitudinal modes ⟨1, 0, 0⟩, ⟨1, 1, 0⟩, and ⟨1, 1, 1⟩ in GaAs with optic polarization for the polarization flipped interaction. Note that the values are much lower than those for the nonflipped interaction.

9.8 DESIGN EXAMPLES

Example 9.5: A/O Interaction with Acoustically Anisotropic Shear Modes. In this example, we analyze the self-collimating Bragg cell, using the rotation matrices. The acoustic mode is the pure shear mode along ⟨1, −1, 0⟩ and polarized along ⟨0, 0, 1⟩. The optic incidence is ⟨1, 1, 1⟩. The matrix $\mathbf{R}_1$ is given by

$$\mathbf{R}_1 = \begin{bmatrix} 1/\sqrt{2} & -1/\sqrt{2} & 0 \\ 1/\sqrt{3} & 1/\sqrt{3} & 1/\sqrt{3} \\ 1/\sqrt{6} & 1/\sqrt{6} & -2/\sqrt{6} \end{bmatrix} \begin{array}{l} \leftarrow \text{acoustic direction} \\ \leftarrow \text{initial optic direction} \\ \end{array}$$

Figure 9.12 shows the effective photoelastic constant as the optic beam is rotated around the acoustic beam. The optic and acoustic polarizations are parallel. In Figure 9.12, $\theta = 0$ corresponds to ⟨1, 1, 1⟩. We see that this direction does not result in the maximum diffracted light. If we rotate

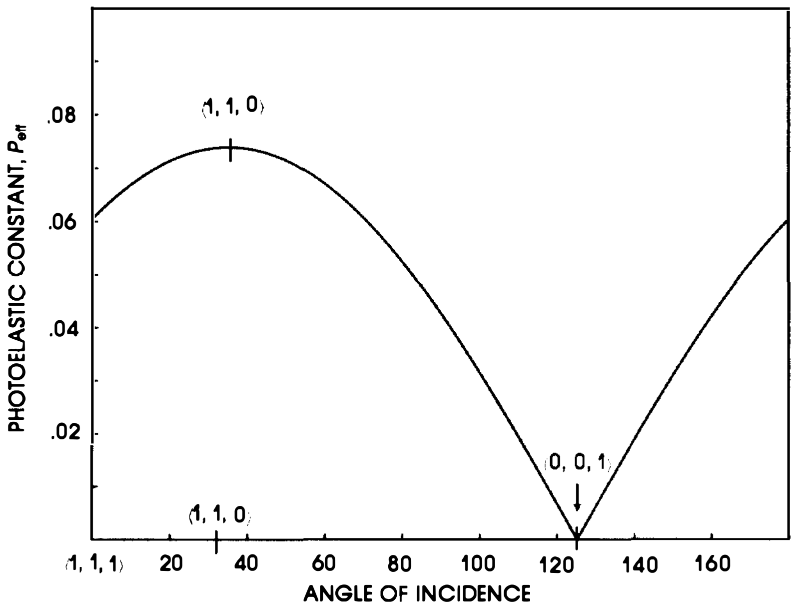

Figure 9.12 Variation of p_{eff} with optic beam incidence for the acoustically anisotropic (self-collimating) interaction in GaP. Note that the interaction is not optimized for this geometry in which the acoustic beam is utilized most effectively (i.e, when $\hat{O}$ = ⟨1, 1, 1⟩).

the beam approximately 35° to the ⟨1, 1, 0⟩ direction, p_{eff} increases significantly. For this direction, however, the *acoustic* beam is not self-collimating. The Bragg bandwidth is the same for both of these optic directions because the acoustic direction (and therefore the acoustic phase velocity) has not changed. For ⟨1, 1, 1⟩, the resolution is higher (larger M_3), but the diffraction efficiency is lower (M_2), whereas for ⟨1, 1, 0⟩ the efficiency increases at the expense of resolution.

The interaction geometry for the acoustically anisotropic device is shown in Figure 9.13. Notice that the acoustic polarization is along ⟨0, 0, 1⟩, which is an eigenmode of the crystal (the fast shear mode), but is at an angle (of about 35°) to the optic face of the device (⟨1, 1, 1⟩). This is accomplished in practice by rotating the transducer to the required angle. The maximum interaction occurs when the optic beam is incident along ⟨1, 1, 0⟩, which is normal to the acoustic polarization. There is no interaction (p_{eff} = 0) when the optic beam is incident along ⟨0, 0, 1⟩ or parallel to the polarization, which makes an angle of 125° with ⟨1, 1, 1⟩ (see Figure 3.4).

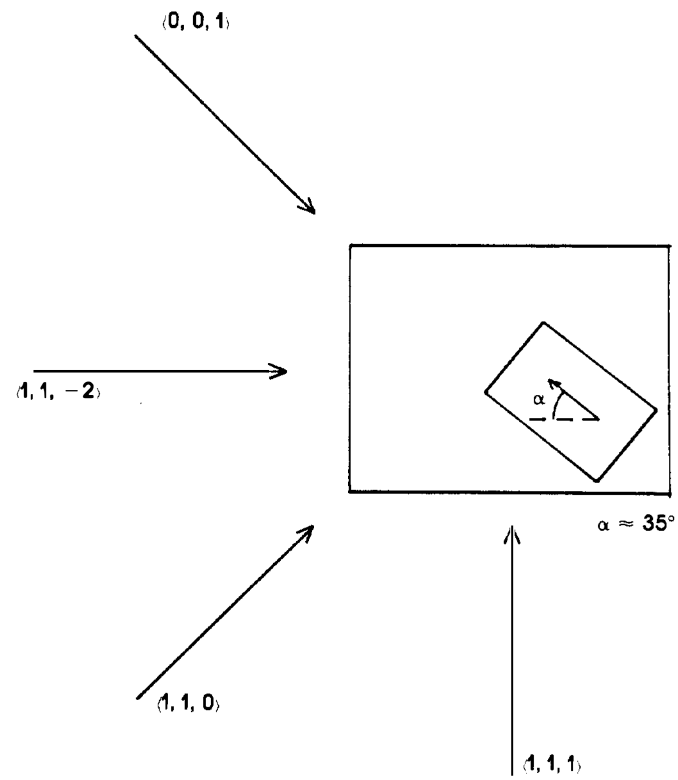

Figure 9.13 Transducer orientation relative to the substrate for the interaction of example 9.5. The angle α is chosen so that the acoustic polarization lies along the $\langle 0, 0, 1\rangle$ (an eigenmode of the substrate).

These results are consistent with Figure 9.3, which indicates that no interaction occurs if the optic beam and acoustic polarization directions are parallel.

Now recall the case of multiple acoustic beams propagating from a single transducer. The geometry of this interaction is shown in Figure 9.14. As in the previous example, the acoustic propagation direction is $\langle 1, 1, 0\rangle$, but the transducer is oriented so that the polarization is parallel to the optic face ($\langle 1, 1, 1\rangle$). Thus there are two orthogonally polarized eigenmodes excited in the substrate lying along $\langle 1, 1, 0\rangle$ and $\langle 0, 0, 1\rangle$. An optic beam incident along $\langle 1, 1, 1\rangle$ interacts with *both* beams. The variation of p_{eff} is

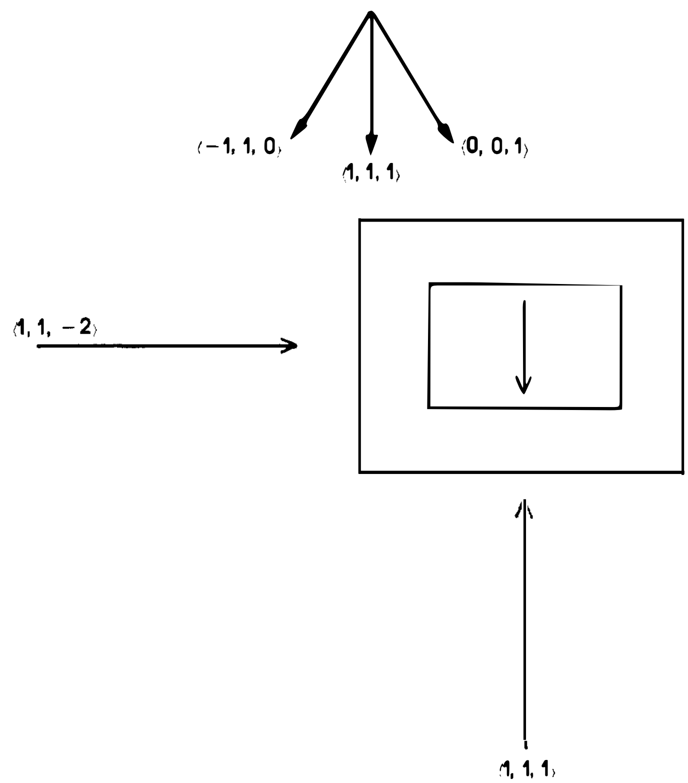

Figure 9.14 Transducer orientation in the configuration in which two acoustic beams are produced from a single transducer. In the example, the acoustic polarization is along ⟨1, 1, 1⟩, which is not an eigenmode of the substrate for $\hat{1}$ along ⟨1, 1, 0⟩.

shown in Figure 9.15. Note that at the direction of optic incidence for which the interaction with the slow mode is maximum (⟨0, 0, 1⟩), there is no interaction with the fast mode, and *vice versa.* This behavior is due to the orthogonality of the eigenmodes. The maximum photoelastic constants for the two modes are equal, but the figures of merit and the bandwidths are not due to the differences in acoustic velocity of the two modes. Note that the Bragg bandwidth as given by (8.8) is valid only for isotropic acoustic modes. In a situation in which the slowness curve bulges out, the diffraction bandwidth can be significantly increased.

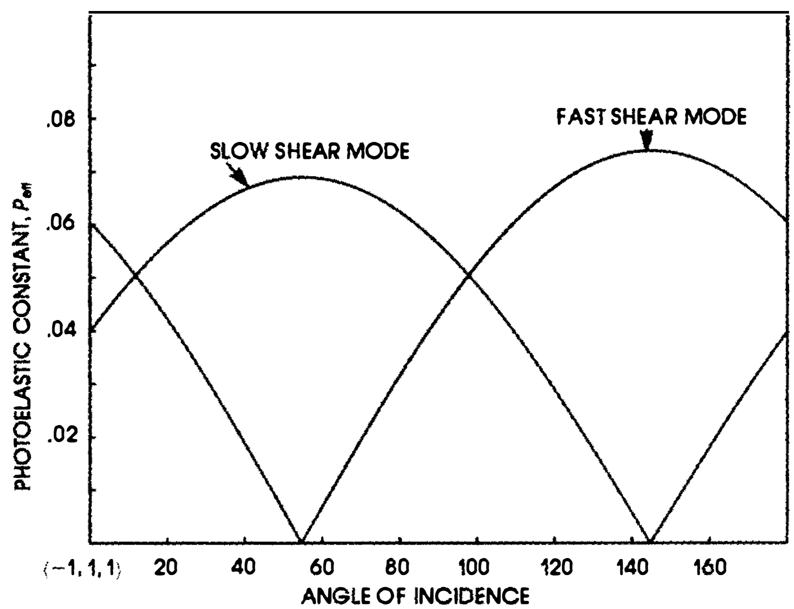

Figure 9.15 Variation of p_{eff} for the two eigenmodes corresponding to the polarization of Figure 9.14. $\theta = 0$ corresponds to $\langle -1, 1, 1\rangle$.

Example 9.6: Design of a Two-Dimensional Beam Deflector. In Example 9.5, we used the $\langle 1, 1, 0\rangle$-directed pure shear mode. In the principal planes, this mode is polarized $\langle 0, 0, 1\rangle$, and the velocity is independent of $\hat{\mathbf{l}}$. The quasishear, on the other hand, is polarized $\langle -1, 1, 0\rangle$. Consider the geometry shown in Figure 9.16. As shown in the figure, both waves in the substrate, which may be either cubic or tetragonal, are quasishear modes because the $\langle 1, 1, 0\rangle$-directed mode is polarized $\langle -1, 1, 0\rangle$ and the $\langle -1, 1, 0\rangle$-directed mode is polarized $\langle 1, 1, 0\rangle$. For a $\langle 0, 0, 1\rangle$-directed optic beam, $\mathbf{R}_l$ has the form:

$$\mathbf{R}_l = \begin{bmatrix} 1/\sqrt{2} & \pm 1/\sqrt{2} & 0 \\ 0 & 0 & 1 \\ 1/\sqrt{2} & \mp 1/\sqrt{2} & 0 \end{bmatrix} \tag{9.33}$$

A $\langle -1, 1, 0\rangle$-polarized optic beam will be flipped into a $\langle 1, 1, 0\rangle$ beam, and a $\langle 1, 1, 0\rangle$ beam will be flipped into a $\langle -1, 1, 0\rangle$ polarization by *either* acoustic beam. A single optic z-directed beam will thus be diffracted into

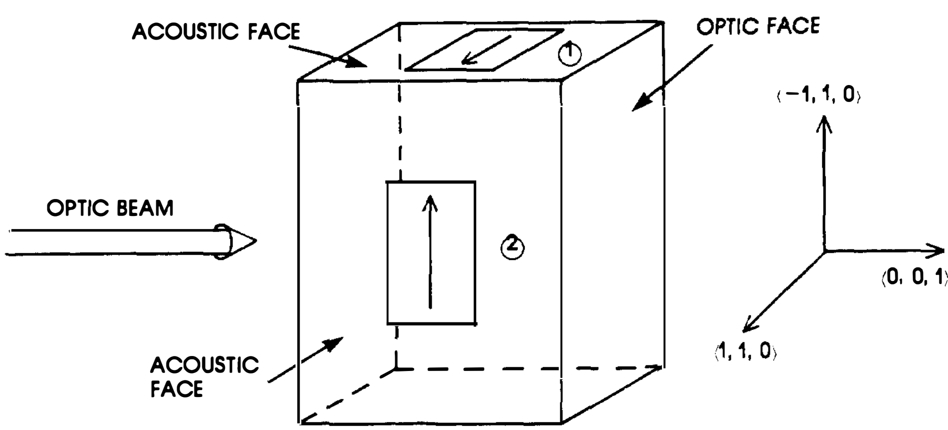

Figure 9.16 Interaction geometry for the two-dimensional beam deflector utilizing the slow shear modes in a cubic system.

two beams orthogonally directed by the two transducers. Curves of the effective photoelastic constant *versus* optic beam direction are shown in Figure 9.17(a) and (b). We see that for a z-directed beam, the two effective constants are maximum and equal.

Example 9.7: Birefringent A/O Interaction in $LiNbO_3$. In Chapter 8, we determined the critical frequency of a birefringent interaction in $LiNbO_3$. The geometry of the interaction is shown in Figure 8.5. Because the acoustic polarization is $\langle 1, 0, 0\rangle$ (the pure shear), the strain simply is:

$$\mathbf{S} = \begin{bmatrix} 0 & 0 & 0 \\ 0 & l_y & 0 \\ 0 & 0 & l_z \\ 0 & l_z & l_y \\ l_z & 0 & 0 \\ l_y & 0 & 0 \end{bmatrix} \begin{bmatrix} 1 \\ 0 \\ 0 \end{bmatrix} = \begin{bmatrix} 0 \\ 0 \\ 0 \\ 0 \\ l_z \\ l_y \end{bmatrix} \tag{9.34}$$

where $l_y = .578$ and $l_z = -.809$ for the interaction, as shown in Figure 8.5. As usual, $\Delta\mathbf{B}$ is given by (9.3). The matrix $\mathbf{R}_1$ is given by

$$\mathbf{R}_1 = \begin{bmatrix} 0 & -.588 & .809 \\ 1 & 0 & 0 \\ 0 & .809 & .588 \end{bmatrix}$$

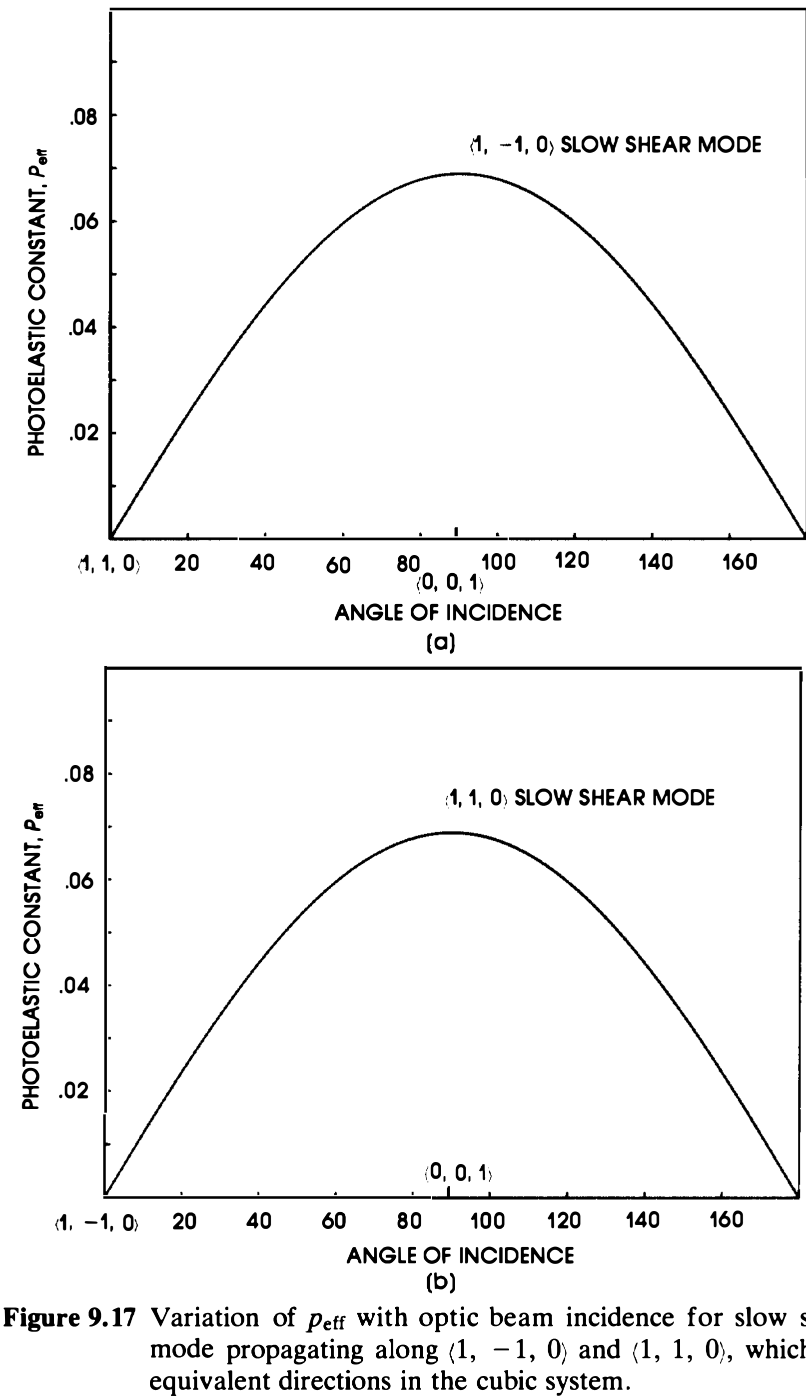

Figure 9.17 Variation of p_{eff} with optic beam incidence for slow shear mode propagating along ⟨1, −1, 0⟩ and ⟨1, 1, 0⟩, which are equivalent directions in the cubic system.

The effective photoelastic constant is shown in Figure 9.18 as a function of optic beam direction. The initial optic incidence direction is along the x-axis. We see that p_{eff} is quite large for this interaction when the optic beam is incident at $y+\ 36°$.

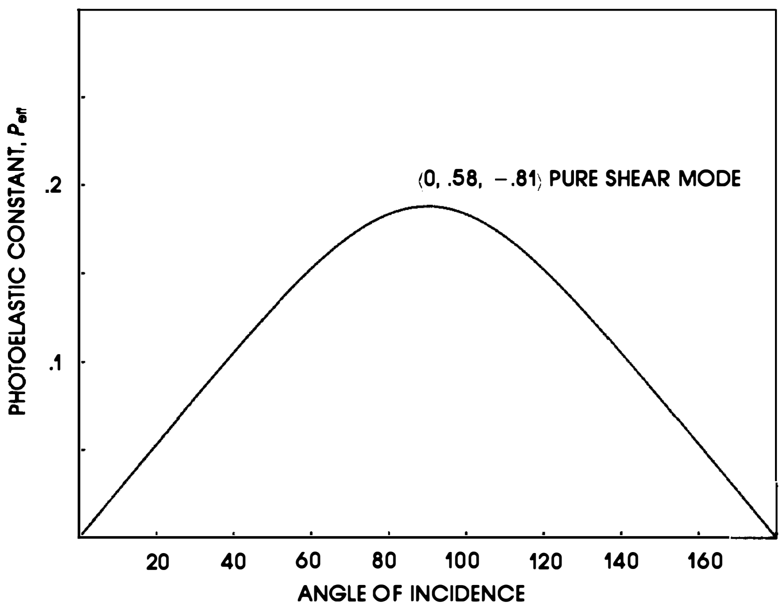

Figure 9.18 Variation of p_{eff} with optic beam incidence for acoustic shear mode with propagation direction of ⟨0, .58, −.81⟩ in which the acoustic polarization is along ⟨x⟩ (pure shear mode). Maximum p_{eff} is close to that of the ⟨x⟩ longitudinal mode interaction (see Figure 9.5).

Example 9.8: Birefringent Interaction in $LiNbO_3$ for Pure Shear Mode in the yz Plane. We have seen in Example 9.4 that for a birefringent interaction there exists an acoustic direction in $LiNbO_3$ (−54° from the $+y$-axis in the yz plane), which yields a very high photoelastic constant when the optic beam is incident along ⟨y⟩ + 36°, i.e., normal to the acoustic polarization. Likewise, p_{eff} is zero for optic incidence along x, i.e., parallel to the acoustic polarization. This behavior is precisely what we would have expected. Historically, this mode of operation was chosen because the crystal faces were identical to those using the traditional ⟨x⟩ longitudinal interaction. In that device, the acoustic direction is ⟨x⟩, with the optic beam incident along ⟨y⟩ + 36°. The performance advantage in terms of deflection efficiency is

$$\frac{\left[p^2/v_a^3\right]_{\text{bir}}}{\left[p^2/v_a^3\right]_{\text{iso}}} = 3.6$$

There is another factor between 4 and 6 (depending on λ_0) due to the birefringence (i.e., the fact that θ_i is stationary near the critical frequency), so the total performance advantage of this mode over the $\langle x \rangle$ longitudinal interaction is about 20. Thus, for a 1-GHz Bragg bandwidth device, we expect a peak efficiency between 30 to 40%/RF W at 633 nm. By decreasing the interaction length, we can significantly increase the Bragg bandwidth while maintaining reasonable diffraction efficiency. A bandwidth of 3 GHz has been achieved with an efficiency of 1%/W at 633 nm [9].

It is clear that for any acoustic propagation in the *yz* plane that utilizes the pure ($\langle x \rangle$ polarized) shear mode the effective photoelastic constant will be a maximum at the optic incidence direction normal to the *x*-axis. In other words, the shape of the p_{eff}-*versus*-θ curve will resemble that of Figure 9.18. It is interesting to determine if a higher value of p_{eff} exists in the *yz* plane. Our task is to form a curve of p_{eff} *versus* angle of *acoustic* propagation with optic incidence normal to the acoustic polarization. Because the optic beam is stationary with respect to the acoustic beam, both $\mathbf{R}_2$ and $\mathbf{R}_3$ are equal to the identity matrix. Because the acoustic polarization is in the *x* direction, **S** is given by (9.34). The matrix $\mathbf{R}_1$ becomes

$$\mathbf{R}_1 = \begin{array}{cl} \begin{bmatrix} 0 & l_y & l_z \\ 0 & -l_z & l_y \\ 1 & 0 & 0 \end{bmatrix} & \begin{array}{l} \leftarrow \text{acoustic direction} \\ \leftarrow \text{optic direction} \\ \end{array} \end{array}$$

$$l_y^2 + l_z^2 = 1$$

The curve of p_{eff} *versus* acoustic propagation direction is shown in Figure 9.19. The angle of maximal interaction occurs at $\langle y \rangle - 65°$ with $p_{\text{eff}} = .228$ (compared with .22 at $\langle y \rangle - 54°$). The phase velocity of this mode is about .5% below that of the $\langle y \rangle - 54°$, so the performance advantage is about 10%. This direction requires that the optic beam be further from the optic axis, so the critical frequency is about 200 MHz higher, which may or may not be an advantage, depending on the application. Table 9.1 summarizes the performance characteristics of presently available wide-bandwidth devices.

Table 9.1

Substrate/Cut	*Mode*	*Efficiency* (% at .63 μm)	f_0 (GHz)	BW (GHz)
$LiNbO_3$/⟨x⟩	Isotropic (long.)	2	1.0	.5
$LiNbO_3$/⟨x⟩	Isotropic (long.)	1	2.0	1.0
$LiNbO_3$ −54° ⟨y⟩	Birefringent (shear)	30	2.3	1.0
GaP/⟨1, 1, 0⟩	Isotropic (long.)	100	1.0	.5
GaP/⟨1, 1, 0⟩	Isotropic (long.)	30	2.0	1.0
GaAs/⟨1, 1, 1⟩	Isotropic (long.)	50 (at 1.06 μm)	1.0	.3
TeO_2/⟨0, 0, 1⟩	Isotropic (long.)	20	1.0	.5

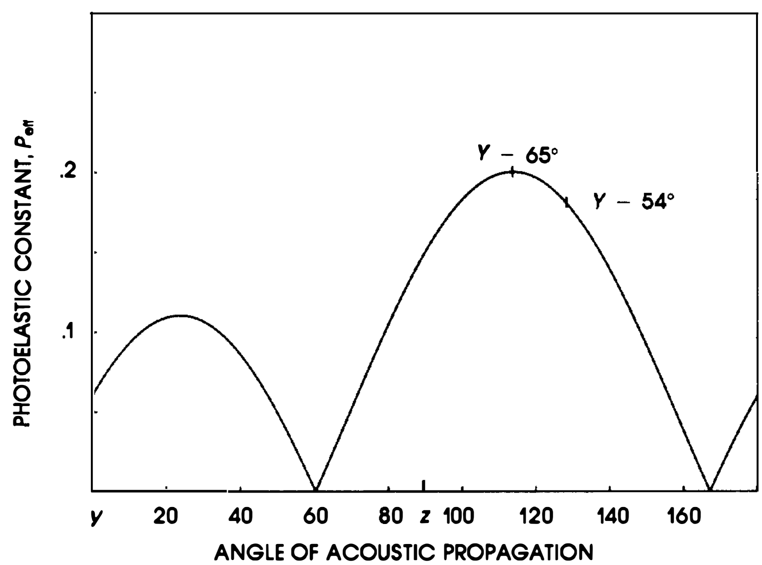

Figure 9.19 Variation of p_{eff} for pure shear mode in the yz plane with direction of acoustic wave. The "standard" (−54° ⟨y⟩) geometry is quite close to the theoretical optimum.

9.9 ELECTRO-OPTIC CORRECTIONS TO THE PHOTOELASTIC MATRIX

As we saw in Chapter 4, in a piezoelectric medium there is a longitudinal field associated with an acoustic wave that propagates at the acoustic velocity. A necessary condition for the existence of the field is that the direction of propagation be piezoactive. The magnitude of the field is

$$\mathbf{E} = -\nabla\phi$$

where the potential ϕ is given by (4.45):

$$\phi = \frac{1}{j\omega}\frac{(l_i e_{iL} l_{Lj})v_j}{l_i \epsilon_{ij}^{S} l_j}$$

In (4.45), recall that the denominator is a scalar, l_i is the acoustic propagation direction, l_{Lj} is the gradient operator, and v_j is the polarization. Using the definition of strain; we write

$$S_L = l_{Lj}u_j = \frac{1}{j\omega}\, l_{Lj}v_j$$

We write the electric field as

$$\mathbf{E} = -\hat{\mathbf{i}}\,\frac{l_i e_{iL} S_L}{l_i \epsilon_{ij}^{S} l_j} \tag{9.35}$$

The acoustically induced electric field interacts with an incident optic beam through the electro-optic effect:

$$\Delta\mathbf{B} = r_{Ij}E_j = \frac{-r_{Ij}l_j l_i e_{iL} S_L}{l_i \epsilon_{ij}^{S} l_j} \tag{9.36}$$

It is important to realize that the electric field in (9.35) is internally generated and propagates at the acoustic velocity and thus behaves exactly like the acoustic wave; i.e., it causes deflection and frequency shifts in the incident optic beam. Comparing (9.36) with (9.3), we write the electro-optically "stiffened" photoelastic components as

$$\Delta\mathbf{B} = p'_{KL}S_L \tag{9.37}$$

where

$$p'_{KL} = p_{KL} - \frac{r_{Ij} l_j l_i e_{iL}}{l_i \epsilon^S_{ij} l_j}$$

Example 9.9: Consider an $\langle x \rangle$-propagating wave in $LiNbO_3$. Find the electro-optically "perturbed" photoelastic matrix.

The unperturbed photoelastic constants are

$$p_{11} = p_{22} = -.03, p_{12} = p_{21} = .09, p_{13} = p_{23} = .13, p_{14} = -.08$$

$$p_{31} = .18, p_{33} = .07, p_{41} = -.15, p_{44} = .15, p_{66} = -.06$$

The piezoelectric and electro-optic matrices have the same form and are given by

$$e_{iL} = \begin{bmatrix} 0 & 0 & 0 & 0 & e_{15} & -e_{22} \\ -e_{22} & e_{22} & 0 & e_{15} & 0 & 0 \\ e_{31} & e_{31} & e_{33} & 0 & 0 & 0 \end{bmatrix}$$

$$r_{Ij} = \begin{bmatrix} 0 & -r_{22} & r_{13} \\ 0 & r_{22} & r_{13} \\ 0 & 0 & r_{33} \\ 0 & r_{51} & 0 \\ r_{51} & 0 & 0 \\ -r_{22} & 0 & 0 \end{bmatrix} \times 10^{-12} \qquad \text{m/V}$$

where

$$e_{15} = 3.7, \qquad e_{31} = .2, \qquad r_{13} = 8.6, \quad r_{33} = 31$$

$$e_{22} = 2.5, \qquad e_{33} = 1.3, \qquad r_{22} = 3.1, \quad r_{51} = 28$$

$$\epsilon_{11} = \epsilon_{22} = 44, \quad \epsilon_{33} = 29,$$

Carrying out the operations in (9.37) gives

$$r_{Ij} l_j = \begin{bmatrix} 0 \\ 0 \\ 0 \\ 0 \\ 2.8 \\ -3.1 \end{bmatrix} \times 10^{-12}, \quad l_i e_{iL} = [0 \quad 0 \quad 0 \quad 0 \quad 3.7 \quad -2.5]$$

Multiplying the 6×1 and 1×6 matrices results in a 6×6 matrix, and dividing by the denominator ($44\epsilon_0$) results in the perturbation matrix;

$$\Delta \mathbf{p} = \begin{bmatrix} 0 & 0 & 0 & 0 & 0 & 0 \\ 0 & 0 & 0 & 0 & 0 & 0 \\ 0 & 0 & 0 & 0 & 0 & 0 \\ 0 & 0 & 0 & 0 & 0 & 0 \\ 0 & 0 & 0 & 0 & -.27 & .18 \\ 0 & 0 & 0 & 0 & .03 & -.02 \end{bmatrix}$$

Note that the perturbation is not symmetric (because the photoelastic matrix is not symmetric). Note that the stiffening terms are present in the shear strains. This is consistent with the fact that $LiNbO_3$ is strongly piezoelectric for $\langle x \rangle$-cut only for the shear mode. Further, the correction terms are as large as, if not larger than, the unperturbed constants! The phenomenon of electro-optic stiffening is not a second-order effect. The strength of the correction terms in the photoelastic matrix and their signs depend on the crystal orientation, acoustic mode, the signs and magnitudes of the piezoelectric and electro-optic matrix components, and the direction and polarization of the optic beam. Because of the complexity of these interactions, it is quite difficult to formulate a general set of rules and a complete determination requires computer aided analysis. A comprehensive search need only focus on crystal orientation and acoustic modes that exhibit strong piezoelectricity: for example, the $\langle x \rangle$ shear and 36° $\langle y \rangle$ longitudinal modes in lithium niobate, and the $\langle z \rangle$ longitudinal mode in barium sodium niobate.

Comparing the forms of (4.46) and (9.36), it is clear that there is a direct analogue between the piezoelectric correction terms in the stiffness matrix and the piezoelectro-optic correction terms in the photoelastic matrix. In both cases, the presence of piezoelectricity alters the propagation characteristics of an acoustic wave. In the stiffness matrix, the uncorrected components are measured under static conditions ($c^{\mathbf{E}}$) so that there is no ambiguity in the determination of the correction terms. The piezoelectro-optic correction is complicated by the fact that the photoelastic matrix components can be measured under static or dynamic conditions. In the static case, the piezo-optic components are measured by applying a stress and then measuring the birefringence using purely optical techniques. In the dynamic case, the acousto-optic diffraction of a particular mode is compared to that of a standard orientation (e.g., fused quartz). Thus, depending on the measured conditions, the piezoelectro-optic corrections may already be "built-in" to the photoelastic matrix.

PROBLEMS

9.1 The components of the photoelastic matrix for water are $p_{11} = p_{12} = .31$. What is the physical meaning of the equality of p_{11} and p_{12}?

9.2 Determine the effective photoelastic constant for the following interactions:

(a) y-propagating longitudinal acoustic wave and optic beam along the z-axis polarized along y in tetragonal symmetry.
(b) x-propagating, y-polarized (shear) acoustic wave and z-incident, y-polarized optic beam in cubic symmetry.
(c) z-propagating, x-polarized acoustic wave and y-incident, x-polarized optic beam in cubic symmetry.

9.3 Find the FOM of the parallel interaction for the z-propagating longitudinal mode in TeO_2. Determine the Bragg bandwidth for a center frequency of 1 GHz and compare the performance of this mode with GaP.

9.4 Write the three transformation matrices $\mathbf{R}_1$, $\mathbf{R}_2$, and $\mathbf{R}_3$ for the following interactions:

(a) acoustic direction: $\langle 1, 1, 1\rangle/\sqrt{3} = \hat{\mathbf{I}}$:
optic incidence: $\langle -2, 1, 1\rangle/\sqrt{6} = \hat{\mathbf{O}}$;
polarization is initially parallel to $\hat{\mathbf{I}}$ and rotates from $\hat{\mathbf{I}}$ to $\hat{\mathbf{O}}$.
(b) acoustic direction: $\langle 1, 1, 1\rangle/\sqrt{3} = \hat{\mathbf{I}}$;
initial optic direction: $\langle -2, 1, 1\rangle/\sqrt{6} = \hat{\mathbf{O}}$;

the optic direction rotates around the acoustic beam.

9.5 Write a computer program that computes the electro-optic perturbation to the photoelastic matrix for piezoelectric crystals.

9.6 Use (9.37) to find the electro-optic perturbation for GaAs (cubic symmetry) for acoustic propagation along $\langle 1, 0, 0\rangle$.

9.7 Consider a two-dimensional beam deflector that uses longitudinal modes instead of the slow shear $\langle 1, 1, 0\rangle$ mode in cubic symmetry. For acoustic propagation along the principal axes, what is the optic polarization required for maximum A/O interaction?

REFERENCES

1. E. Spencer, P. Lenzo, and A. Ballman, "Dielectric Materials for Electo-Optic, Elasto-Optic and Ultrasonic Device Applications," *Proc. IEEE*, **55** (12), 2074 (1967).
2. Y. Gulyaev, V. Proklov, and G. Shkerdin, "Diffraction of Light by Sound in Solids," *Sov. Phys. Usp.* **21** (1), 29 (1978).
3. D. Pinnow, "Guide Lines for the Selection of Acousto-Optic Materials," *IEEE J. Quantum Electron.* **QE-6** (3), 223 (1970).
4. R. Dixon, "Photoelastic Properties of Selected Materials and Their Relevance for Applications to Acoustic Light Modulators and Scanners," Applied Physics **38** (12), 5149 (1967).
5. L. Avakyants, D. Kiselev, and N. Shchitov, "Photoelasticity of $LiNbO_3$," *Sov. Phys. Solid State* **18** (6), 899 (1976).
6. R. Brazhe, M. Grigor'ev, and V. Nayanov, "Efficiency of Light Diffraction by Pure Elastic Wave Modes," *Sov. Phys. Solid State* **17** (3), 562 (1975).
7. R. Dixon and M. Cohen, "A New Technique for Measuring Magnitudes of Photoelastic Tensors and its Application to Lithium Niobate, *Applied Physics Letters*, **8,** 205 (1966).
8. P. Wasilousky, *et al.*, "High Performance Wideband Bragg Cells for EW Processing," *Proc. SPIE* (1985).
9. J. Poncot, *et al.*, "3-GHz Bandwidth Bragg Cells," *Proc. 1987 IEEE Ultrasonics Symposium*, 501 (1987).
10. J. Bagnhaw and T. Willats, "Anisotropic Bragg Cells," *GEC J. Res.*, **2,** 96 (1984).